Ruthenium(II) Porphyrin Quinoid Carbene Complexes: Synthesis, Crystal Structure and Reactivity Towards Carbene Transfer and Hydrogen Atom Transfer Reactions

Hai-Xu Wang,[†] Qingyun Wan,[†] Kai Wu,[†] Kam-Hung Low,[†] Chen Yang,[†] Cong-Ying Zhou,[†] Jie-Sheng Huang,[†,*] and Chi-Ming Che[†,‡,*]

[†] State Key Laboratory of Synthetic Chemistry and Department of Chemistry, The University of Hong Kong, Pokfulam Road, Hong Kong SAR, China

[‡] HKU Shenzhen Institute of Research & Innovation, Shenzhen, China

ABSTRACT: Reactivity study of novel metal carbene complexes can offer new opportunities in catalytic carbene transfer reactions as well as in other synthetic protocols. Metal complexes with quinoid carbene (QC) ligands are assumed to be key intermediates in a variety of metal-catalyzed QC transfer reactions using diazo quinones, which demands development of the chemistry of QC transfer of well characterized metal-QC complexes. Herein we report the isolation and QC transfer of ruthenium porphyrins [Ru(Por)(QC)] which contribute the first examples of (i) structurally characterized metal-QC complex (by X-ray crystallography) and (ii) isolated metal-QC complex that undergoes QC transfer reaction. The complexes [Ru(Por)(QC)] were prepared from reaction of [Ru(Por)(CO)] with diazo quinones and exhibited dual reactivity, i.e. hydrogen atom transfer (HAT) as well as QC transfer. The stoichiometric QC transfer reactions from these Ru-QC complexes to nitrosoarenes (ArNO) afforded nitrones in up to 90% yield, and the corresponding catalytic reactions were also developed. Both the stoichiometric and catalytic reactions for a series of QC ligands bearing electron-donating and -withdrawing substituents showed a reverse substituent effect on the QC transfer reactivity. Complexes [Ru(Por)(QC)] are also reactive towards C–H and X–H (X = N, S) bonds and can catalyze aerobic oxidation of 1,4-cyclohexadiene; their stoichiometric HAT reactions with unsaturated hydrocarbons gave product yields of up to 88%. The unique dual reactivity and electronic feature of [Ru(Por)(QC)] were studied by spectroscopic means and density functional theory (DFT) calculations.

■ INTRODUCTION

Isolation and reactivity studies of metal carbene complexes are fundamental to the rapid development and mechanism elucidation of metal-carbene-based methodologies[1,2] such as metal-catalyzed carbene transfer reactions which have enjoyed wide applications in practical organic synthesis. A number of isolated metal carbene complexes that undergo carbene transfer reactions have been reported.[3,4] These complexes bear alkoxy, alkoxycarbonyl or aryl carbenes such as C(Ar)CO$_2$R and CAr$_2$. Conjugated carbenes based on carbocyclic backbone have been attracting increasing attention in metal-catalyzed carbene transfer reactions. Notable examples include Rh-catalyzed alkene cyclopropanation recently reported by Baran and co-worker[5] as well as a variety of catalytic processes using diazo quinones (also called quinone diazides),[6,7,8,9] the key intermediates in which are generally proposed to be metal complexes of the corresponding carbene, herein called quinoid carbene (QC). These proposed M-QC species in the catalytic processes were assumed to undergo QC transfer to various organic targets including C–H bond,[7] alkene,[5,8] O–H bond,[9a,f] anhydride,[9b] enol ether,[9c] cyclic ether,[9d] and halide[9e] (Figure 1a). Quinoid carbenes (QCs), previously named oxocyclohexadienylidenes[10] or cyclohexadienone carbenes,[5] are electrophilic and feature delocalized π-system;[10] their metal com-

plexes may exhibit unique properties/reactivities compared with other carbenes. Milstein and co-workers isolated and spectroscopically characterized a ruthenium-QC complex[11a] and subsequently an iron counterpart,[11b] and describe the two complexes as metallaquinones, without observation of QC transfer to organic substrates (Figure 1a, inset). In addition, the two metallaquinones, termed ruthenaquinone and ferraquinone, were not generated from reactions with diazo quinones; formation of both the ruthenaquinone and ferraquinone requires chelating auxiliary groups and terminal CO co-ligands, and reactivity studies were performed to the ferraquinone revealing its reactions with H$_2$, Br$_2$, alcohols and acid to form ferrahydroquinones.[11b] On the other hand, the proposed metal-QC intermediates in the catalytic reactions[5,7-9] have not been isolated nor directly detected by spectroscopic means.[12] Thus, challenges remain to address the following issues about metal-QC complexes: (i) clear observation of their formation from reaction with diazo quinones, (ii) examination of their intrinsic stability or isolation of their examples devoid of chelating auxiliary group(s), (iii) elucidation of their structure features by X-ray crystallographic studies, and (iv) exploration of their novel reactivities, particularly the possibility of QC transfer.

In the present paper, we aim to address these issues by isolation of ruthenium porphyrin QC complexes [Ru(Por)(QC)] from reaction of [Ru(Por)(CO)] (Por = porphyrinato dianion)
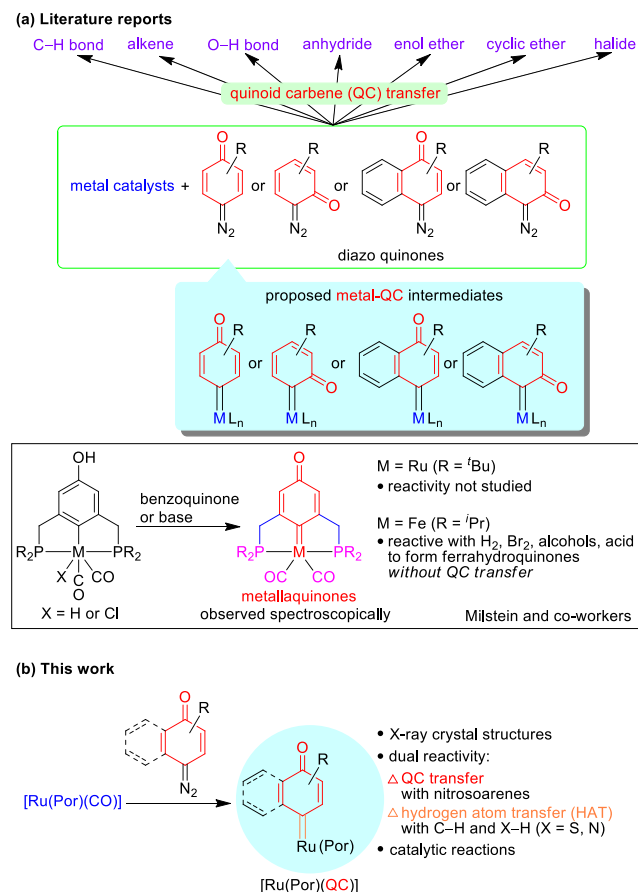
(a) Literature reports

C–H bond · alkene · O–H bond · anhydride · enol ether · cyclic ether · halide

quinoid carbene (QC) transfer

metal catalysts + (diazo quinones)

diazo quinones

proposed metal-QC intermediates

M = Ru (R = ^{t}Bu)
• reactivity not studied

M = Fe (R = ^{i}Pr)
• reactive with H$_2$, Br$_2$, alcohols, acid to form ferrahydroquinones *without QC transfer*

metallaquinones
observed spectroscopically

X = H or Cl

Milstein and co-workers

(b) This work

[Ru(Por)(CO)] → [Ru(Por)(QC)]

• X-ray crystal structures
• dual reactivity:
△ QC transfer with nitrosoarenes
△ hydrogen atom transfer (HAT) with C–H and X–H (X = S, N)
• catalytic reactions

Figure 1. (a) Literature reported examples of "metal catalyst + diazo quinone" systems for catalytic quinoid carbene (QC) transfer to various organic groups/substrates via proposed metal-QC intermediates.[5–9] Inset: Spectroscopically observed metallaquinones reported by Milstein and co-workers.[11] (b) Structurally characterized ruthenium porphyrin QC complexes reported in this work, which are formed from reaction with diazo quinones and exhibit QC transfer and hydrogen atom transfer (HAT) dual reactivity.
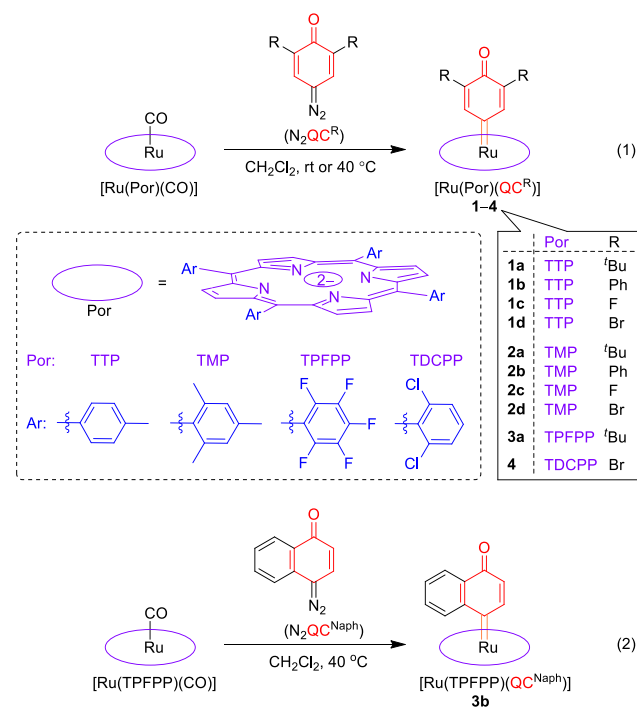
with diazo quinones, along with structure characterization, reactivity, catalytic, and mechanistic studies (Figure 1b), including DFT calculations. The Ru-QC complexes isolated in this work have been characterized by X-ray crystal structure determination, as well as by spectroscopic means; strikingly, they exhibit a dual reactivity, i.e. QC transfer as well as quinone-like hydrogen atom transfer (HAT), and their QC transfer reactions with a nucleophile was retarded by electron-withdrawing substituent (but accelerated by electron-donating substituent) on the carbene ligand, which is an "inverted" electrophilicity/reactivity order compared with that reported previously for free QCs[10a] and isolated metal complexes of electrophilic carbenes.[4e,g,13,14]

■ RESULTS

Synthesis. In exploration of a synthetic route to a metal complex with non-chelating QC ligand (unlike the pincer-type chelating QC ligand in the metallaquinones reported by Milstein and co-workers[11]), we focused on porphyrin auxiliary ligand systems in view of their ability to support isolable metal complexes with other types of carbenes including C(Ar)CO$_2$R and CAr$_2$[4,15] along with transfer of such carbenes[1f,k,r,15] and

dialkylcarbenes[16] catalyzed by metalloporphyrins. Also, we used the same type of QC source as that in the catalytic processes,[5,7-9] i.e. diazo quinones. Diazo compounds are well documented to coordinate with metal ions;[17] however, previous reports on the stoichiometric reactions of metal complexes with diazo quinones are rare,[18] which resulted in the formation of diazo quinone complexes of rhodium(I)[18b] and iridium(I)[18a] without observation of the corresponding metal-QC complexes.

Scheme 1. Syntheses of Ruthenium Porphyrin Quinoid Carbene Complexes 1–4

	Por	R
1a	TTP	^{t}Bu
1b	TTP	Ph
1c	TTP	F
1d	TTP	Br
2a	TMP	^{t}Bu
2b	TMP	Ph
2c	TMP	F
2d	TMP	Br
3a	TPFPP	^{t}Bu
4	TDCPP	Br

Interestingly, treatment of [Ru(Por)(CO)] with diazo quinones N$_2$QC^R (2,6-disubstituted 4-diazocyclohexa-2,5-dienones) in CH$_2$Cl$_2$ at 40 °C or room temperature afforded Ru-QC complexes [Ru(Por)(QC^R)] (Por = TPP, **1a–d**; TMP, **2a–d**; TPFPP, **3a**; TDCPP, **4**) in 35–92% yields (reaction 1, Scheme 1). While **1b–d** were only stable in solutions for ~4 h at room temperature, the other complexes generally exhibited good stability and showed no sign of decomposition in solutions at room temperature for around one week. Other types of diazo quinones, such as 4-diazonaphthalen-1(4*H*)-one (N$_2$QC^{Naph}), can also react with [Ru(Por)(CO)] to afford Ru-QC complexes. For example, treatment of [Ru(TPFPP)(CO)] with N$_2$QC^{Naph} in CH$_2$Cl$_2$ at 40 °C gave [Ru(TPFPP)(QC^{Naph})] (**3b**, 32% yield, reaction 2 in Scheme 1), which is only stable for ~1 d in solution.

X-ray Crystal Structures. Slow evaporation of a hexane-AcOEt solution of **1a**, layering MeOH over a CH$_2$Cl$_2$ solution of **2d**, or slow evaporation of a hexane-CH$_2$Cl$_2$-^{n}BuOCH$_2$CH$_2$OH solution of **3a** gave diffraction-quality crystals of **1a**·AcOEt, **2d**·MeOH, or **3a**·^{n}BuOCH$_2$CH$_2$OH, respectively, the structures of which were determined by X-ray crystallography (Figure 2). These Ru-QC complexes each adopt an octahedral coordination geometry with a sixth O-donor ligand (AcOEt, MeOH, or ^{n}BuOCH$_2$CH$_2$OH for **1a**, **2d**, or **3a**, respectively).
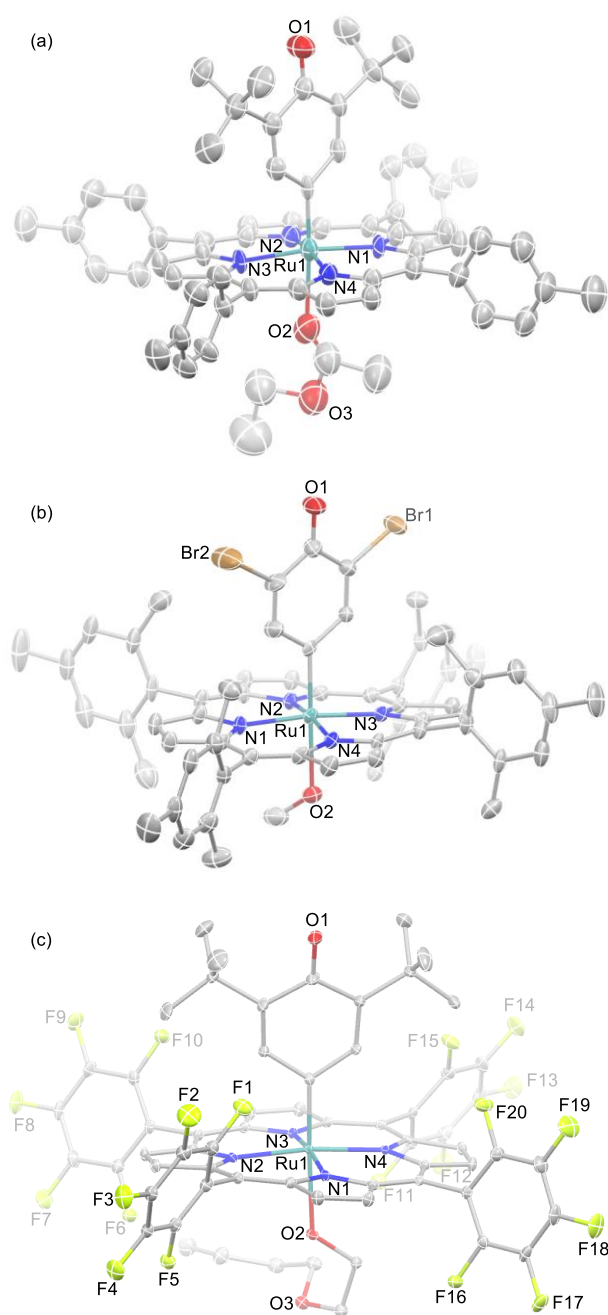
2

Figure 2. *ORTEP* diagrams of (a) **1a**·AcOEt, (b) **2d**·MeOH, and (c) **3a**·*^{n}*BuOCH$_2$CH$_2$OH with thermal ellipsoids at 30% probability level. Hydrogen atoms are not shown.

The Ru–C$_{carbene}$ distance in [Ru(TTP)(QC^{tBu})] (**1a**) is 1.841(9) Å, which is similar to the typical Ru–C$_{carbene}$ distances previously reported for ruthenium porphyrins bearing CHCO$_2$R, C(CO$_2$R)$_2$, C(COAr)$_2$, C(Ph)CO$_2$R, or CAr$_2$ carbene ligands (1.806(3)–1.877(8) Å).[4b,f, 19, 20] Compared with **1a**, complexes [Ru(TMP)(QC^{Br})] (**2d**) and [Ru(TPFPP)(QC^{tBu})] (**3a**) show longer Ru–C$_{carbene}$ distances of 1.922(8) and 1.915(3) Å, respectively; this might be associated with the larger steric hindrance of the TMP (see Figure S1 in the Supporting Information) and TPFPP ligands and/or the electron-withdrawing substituents in QC^{Br} and TPFPP (see Discussion section). The Ru–O distances in **2d** and **3a** (2.264(6) and 2.2945(19) Å,

respectively) are shorter than that in **1a** (2.358(10) Å), possibly reflecting reduced *trans* influence of the carbene ligands in **2d** and **3a**. For all of **1a**, **2d**, and **3a**, their Ru–C$_{carbene}$ distances (1.841(9)–1.922(8) Å) are significantly shorter than the Ru–C$_{aryl}$ distance (2.121(6) Å) in the zwitterionic Ru-aryl counterpart of the ruthenaquinone (Figure 3, inset C).[11a]

The coordinated QC ligands in **1a**, **2d**, and **3a** feature a cyclohexadienone moiety similar to that of related quinones, as revealed by comparison with the X-ray crystal structures of two di(*tert*-butyl)-substituted 1,4-benzoquinones[21] (Figure 3, insets A and B). The quinoid structures of the QCs in **1a**, **2d**, and **3a** contrast with the benzenoid structure in the zwitterionic Ru-aryl counterpart of the ruthenaquinone (Figure 3, inset C).[11a] Worthy of note is that the C=O group of each QC ligand is co-planar with the carbene plane, unlike the cases of common α-carbonyl carbenes such as C(Ar)CO$_2$R in which the C=O group tilts ~60° away from the carbene plane[20a,c] (see, for example, Figure 3, inset D, and also the results from DFT calculations).
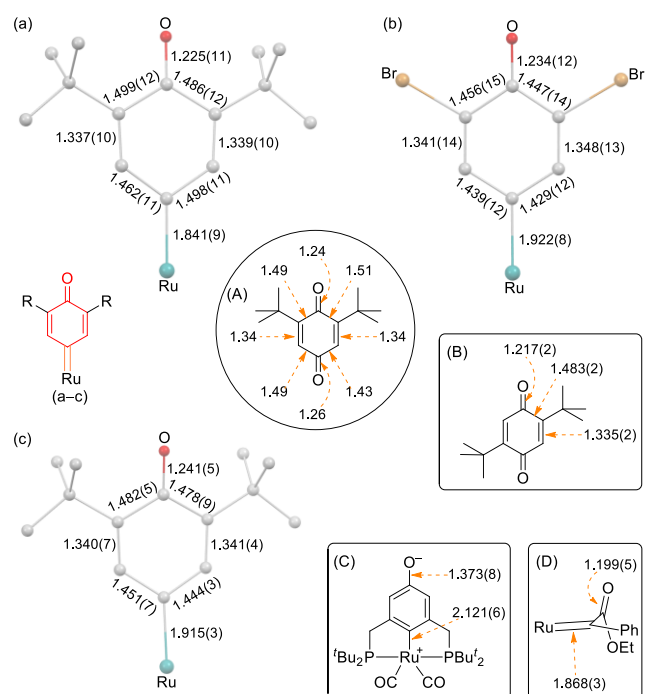

Figure 3. Bond distances (Å) for the Ru-QC moieties in the crystal structures of (a) **1a**·AcOEt, (b) **2d**·MeOH, and (c) **3a**·*^{n}*BuOCH$_2$CH$_2$OH. Insets: bond distances (Å) in the X-ray crystal structures of two related quinones (A and B; standard errors not available for A; only the average C=O, C–C, C=C distances are reported for B)[21] and selected bond distances (Å) in the X-ray crystal structures of zwitterionic form of the ruthenaquinone[11a] (C) and [Ru(TPFPP)(C(Ph)CO$_2$Et)(MeOH)][20c] (D).

In the crystal structures of **1a**, **2d** and **3a**, their QC carbene planes make angles of ~29°, ~19°, and ~4°, respectively, with the closest pair of diagonal Ru–N bonds (Figure S2; the corresponding angles reported for ruthenium porphyrins bearing other types of carbene ligands are ~2°–39°[20c]). The porphyrin rings in **1a**, **2d** and **3a** show slight saddle (**1a**) or ruffle (**2d** and **3a**) distortions (Figure S2, inset) and the ruthenium atoms are displaced from the mean porphyrin planes by 0.220, 0.140 and 0.165 Å, respectively.

Spectral Features. Complexes **1–4** (in CDCl$_3$ or CD$_2$Cl$_2$)

exhibited well-resolved ^{1}H NMR signals in the diamagnetic region (see the Supporting Information). All the protons on their QC ligands were shielded due to the ring current effect of the porphyrin macrocycles (e.g. the signals of the C–H protons α to carbene carbons appear at δ 0.72–2.05 ppm). The H$_\beta$ (pyrrolic protons) signals of their porphyrin ligands appear at δ 8.31–8.35 (TTP in **1a–d**), 8.07–8.12 (TMP in **2a–d**), 8.35–8.42 (TPFPP in **3a,b**), and 8.16 ppm (TDCPP in **4**), similar to those of other ruthenium porphyrin carbene complexes (e.g. δ 8.36, 8.13, 8.32, 8.27 ppm for [Ru(TTP)(CPh$_2$)], [Ru(TMP)(CPh$_2$)], [Ru(TPFPP)(CPh$_2$)], [Ru(TDCPP)(CPh$_2$)], respectively[20]).

The ^{13}C NMR spectra were measured for **1a**, **2a–d**, and **3a,b** (in CDCl$_3$ or CD$_2$Cl$_2$; the other complexes were not sufficiently stable (in solution) or soluble), each featuring two downfield signals (δ 245.12–287.19 and 183.35–198.28 ppm) which could be assigned to Ru=C and C=O carbons, respectively. The Ru=C chemical shifts of **1a**, **2a,b**, **3a**, and **3b** (δ 260.10–287.19 ppm) are comparable to those of porphyrin-supported Ru=C(CO$_2$R)$_2$ (δ 271.36–280.49 ppm)[4b,20c] and Ru=CHCO$_2$Ar (δ 281.30 ppm, Ar = 2,6-^{t}Bu-4-Me-C$_6$H$_2$)[19] complexes but appreciably smaller than those of the non-porphyrin-supported ruthenaquinone (δ 303.08 ppm)[11a] and porphyrin-supported Ru=CAr$_2$ (δ 316.30–346.69 ppm)[20c] counterparts. Complexes **2c,d** bearing electron-withdrawing F and Br substituents, respectively, on their QC ligands show appreciably smaller Ru=C chemical shifts (δ 248.45, 245.12 ppm). For [Ru(Por)(QC^{tBu})] (**1a**, **2a**, **3a**), the Ru=C chemical shift follows an order **2a** (Por = TMP, δ 271.06 ppm) < **1a** (Por = TTP, δ 274.79 ppm) < **3a** (Por = TPFPP, δ 287.19 ppm).

In the UV-vis spectra of **1–4** in CH$_2$Cl$_2$ (Figure S3 in the Supporting Information), the Soret bands appear at λ_{max} 407–411 nm (**1a–d**), 405–410 nm (**2a–d**), 401–403 (**3a,b**), and 406 nm (**4**). No appreciable solvatochroism was observed by changing the solvent to MeOH or acetone, unlike the ruthenaquinone[11a] (Figure 1, inset) which exists in benzene or THF solution but, when dissolved in methanol or acetone, changes color and transforms to the zwitterionic Ru-aryl form (Figure 3, inset C).

Electrochemistry. Coordinated QCs in metal-QC complexes constitute a unique type of redox noninnocent carbene ligands in view of the ferraquinone-ferrahydroquinone couple revealed by chemical oxidation/reduction reactions.[11b] However, the redox behaviors of metal-QC complexes, including metallaquinones, under electrochemical conditions remain unexplored.

We measured the cyclic voltammograms of [Ru(Por)(QC^R)] complexes **1a**, **2a–d** and **3a** in CH$_2$Cl$_2$ (Figure 4; Figure S4 in the Supporting Information); the redox potentials are compiled in Table 1. These complexes generally exhibit three reversible or quasi-reversible redox waves: two reduction waves (E_{R1} and E_{R2} represented by $E_{1/2}$) and one oxidation wave (E_{O1} represented by $E_{1/2}$). An extra oxidation wave (quasi-reversible or irreversible, $E_{1/2}$ or E_{pa} represented by E_{O2}) was observed for [Ru(TMP)(QC^R)] (**2a–d**) bearing electron-rich TMP ligand. For comparison, we also measured the cyclic voltammograms of [Ru(Por)(CO)] (Por = TTP, TMP) under similar conditions (Figure S4 in the Supporting Information); these Ru-carbonyl porphyrins have been studied in detail by cyclic voltammetry.[22]

The E_{O1} values of [Ru(Por)(QC^{tBu})] are 0.28, 0.48, and 0.54 V vs Fc$^{+/0}$ for Por = TMP (**2a**), TTP (**1a**), and TPFPP (**3a**), respectively, and [Ru(TMP)(QC^R)] gave E_{O1} values (V vs Fc$^{+/0}$) of 0.28 (R = ^{t}Bu, **2a**), 0.37 (R = Ph, **2b**), 0.52 (R = F, **2c**), and 0.53 (R = Br, **2d**). These observations indicate increase of E_{O1} values with weaker electron-donating, or stronger electron-withdrawing, substituents on the porphyrin and/or QC ligands. These E_{O1} values (0.28–0.54 V vs Fc$^{+/0}$) fall in the range of E_{O1} values observed for the first oxidation waves of ruthenium porphyrin complexes bearing other types of carbene ligands (0.19–0.77 V vs Fc$^{+/0}$).[20c] For [Ru(TTP)(QC^{tBu})] (**1a**) and [Ru(TMP)(QC^R)] (R = ^{t}Bu, Ph; **2a**, **2b**), their E_{O1} values are similar to those measured for [Ru(TTP)(CO)] (0.50 V vs Fc$^{+/0}$) and [Ru(TMP)(CO)] (0.32 V vs Fc$^{+/0}$), respectively, under similar conditions. Spectroelectrochemistry of **2b** in CH$_2$Cl$_2$ at 0.85 V vs Ag/AgCl (Figure 5) revealed that the first oxidation caused a marked change of its UV-vis spectrum, with isosbestic points at 354, 432, 486, and 612 nm, together with appearance of a band in the 600–700 nm region characteristic of porphyrin-centered oxidation,[23] resembling the first oxida-
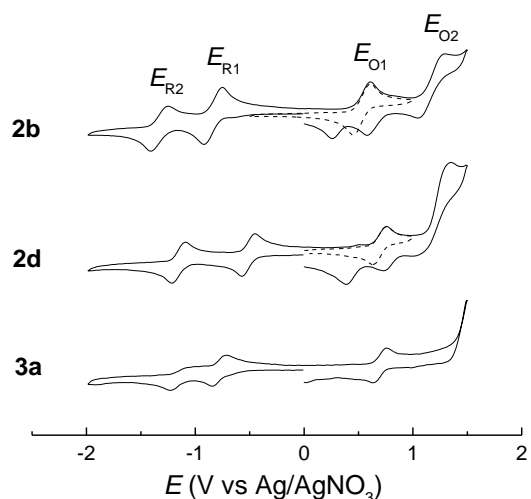

Figure 4. Cyclic voltammograms of **2b**, **2d**, and **3a** in CH$_2$Cl$_2$ (V vs Ag/AgNO$_3$) with 0.1 M (^{n}Bu$_4$N)PF$_6$ as electrolyte and at a scan rate of 0.1 V s^{-1}.

Table 1. Redox Potentials V vs Ag/AgNO$_3$ (Values in Parenthesis: V vs Fc$^{+/0}$)^a

complex	E_{O1}	E_{O2}	E_{R1}	E_{R2}	$E(Fc^{+/0})$
1a	0.65		−1.00	−1.39	0.17
	(0.48)		(−1.17)	(−1.56)	
2a	0.44	1.13	−1.10	−1.50	0.16
	(0.28)	(0.97)	(−1.26)	(−1.66)	
2b	0.53	1.17	−0.83	−1.33	0.16
	(0.37)	(1.01)	(−0.99)	(−1.49)	
2c	0.68	1.18	−0.59	−1.17	0.16
	(0.52)	(1.02)	(−0.75)	(−1.33)	
2d	0.69	1.35^b	−0.51	−1.15	0.16
	(0.53)	(1.00)	(−0.67)	(−1.31)	
3a	0.70		−0.78	−1.14^b	0.16
	(0.54)		(−0.94)	(−1.30)	

$^a E_{1/2}$ values. ^{b}Irreversible (E_{pa}).

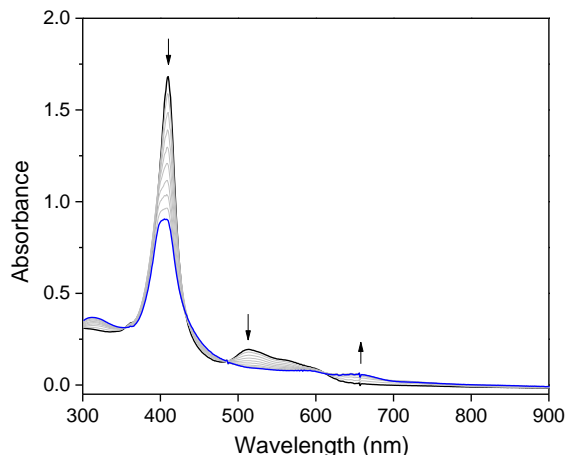**Figure 5**. Spectroelectrochemistry of **2b** in CH_2Cl_2 with 0.1 M ($^{n}Bu_4N$)PF_6 as electrolyte at 0.85 V vs Ag/AgCl.

tion of [Ru(TMP)(CO)] attributed to porphyrin-centered process.[22b,c]

The two reduction waves of [Ru(Por)(QC^R)] are reminiscent of two sequential 1 e$^−$ reductions of quinones such as 1,4-benzoquinone in aprotic organic solvents,[24] and occur at potentials (E_{R1} and E_{R2}) which, particularly E_{R1}, are considerably less cathodic than the potentials for the first reduction waves of the corresponding [Ru(Por)(CO)] complexes (see Figure S4) and also the porphyrin-supported ruthenium[20c] or iron[25] complexes with other types of carbene ligands.[20c] These two reductions, at least the first reduction, of [Ru(Por)(QC^R)] could be ascribed to be essentially the QC-ligand centered, consistent with the finding that the E_{R1} values of [Ru(Por)(QC^R)] are markedly less cathodic for the QC^R ligands bearing weaker electron-donating, or stronger electron-withdrawing, substituents (cf. E_{R1} of [Ru(TMP)(QC^R)]): −1.26, −0.99, −0.75, −0.67 V vs Fc$^{+/0}$ for R = ^{t}Bu (**2a**), Ph (**2b**), F (**2c**), Br (**2d**), respectively). Reducing the electron density of the Por ligands in [Ru(Por)(QC^{tBu})] also leads to less cathodic E_{R1} values (−1.26, −1.17, −0.94 V vs Fc$^{+/0}$ for Por = TMP (**2a**), TTP (**1a**), and TPFPP (**3a**), respectively).

Binding Behavior towards Pyridines and Imidazoles. [Ru(Por)(QC^R)] complexes could form adducts with N-donor ligands such as pyridine and 1-methylimidazole. These adducts were found to be only stable for ~3 h in solution and were susceptible to QC dissociation and degradation; for instance, treatment of **2b** with excess pyridine gave [Ru(TMP)(Py)$_2$] (and 2,6-diphenyl-*p*-benzoquinone) after the reaction mixture had been left standing overnight, analogous to the formation of [Ru(TPP)(Py)$_2$] from treatment of [Ru(TPP)(CHCO$_2$Ar)(THF)] with pyridine.[19]

The formation of adduct [Ru(TMP)(QC^{Ph})(Py)] (**2b·Py**) from [Ru(TMP)(QC^{Ph})] (**2b**) led to a red shift of the Soret band in the UV-vis spectrum (Figure S5), like the case of [Ru(TPFPP)(CPh$_2$)] vs [Ru(TPFPP)(CPh$_2$)(Py)].[20c] Interestingly, complex **2b** showed preference for the binding with pyridines and 1-methylimidazole, as revealed by their large binding constants (K_L) with **2b** (Table S5), while formation of six-coordinate products with PPh$_3$ or PhNO ligand could not be detected by UV-vis and ^{1}H NMR monitoring.

Dual Reactivity. (i) Stoichiometric and Catalytic QC Transfer Reactions with Nitrosoarenes. The isolation of [Ru(Por)(QC)] complexes allows direct exploration of carbene transfer reactivity of metal complexes of non-chelating QCs towards organic substrates. As metal-catalyzed QC transfer reactions of diazo quinones[5-9] are not known for Ru catalysts, we intended to find a type of organic compounds to which a Ru-mediated QC transfer can occur, and then to develop the corresponding Ru-catalyzed QC transfer reactions.

Nitrosoarenes are the candidates of choice in this work, based on the following considerations: In our reports on ruthenium porphyrin-catalyzed three-component reactions for synthesis of isoxazolidines [26 a] or aziridines,[26b,c] the proposed mechanisms involve carbene transfer of porphyrin-supported Ru=CHX (X = CO$_2$Et, C(O)Ar, P(O)(OMe)$_2$, C$_n$F$_{2n+1}$) intermediates to nitrosoarenes to in situ generate nitrone intermediates,[26,27] but isolation of those nitrone intermediates (one of which was observed spectroscopically[26a]) was hampered by their relatively poor stability. In fact, we are aware of no previous examples of reaction of isolated metal-carbene complexes with nitrosoarenes to give isolated nitrones. As nitrones possessing QC moieties are quite stable and isolable,[28] the QC transfer from [Ru(Por)(QC)] to nitrosoarenes, if occurs, would not only demonstrate the QC transfer reactivity of an isolated metal-QC complex but also facilitate mechanistic studies on the nitrone formation from a metal-carbene complex with nitrosoarenes.

Interestingly, treatment of **1a–d** with excess nitrosoarenes (PhNO and its *para*-substituted derivatives) at room temperature resulted in QC transfer to the nitrosoarenes, affording nitrones **5a–h** in high isolated yields (75–90%, Table 2). A similar treatment of **3b** with PhNO gave nitrone **5i** in 77% yield (Scheme 2). All these nitrone products were characterized by NMR and HRMS, and for **5d** its crystal structure was determined by X-ray crystallography (Figure 6). The fate of the Ru-QC complexes after QC transfer was exemplified by the reactions of **1a–d** with PhNO affording [Ru(TTP)(PhNO)$_2$], a previously reported Ru(II)-nitrosoarene complex.[29]
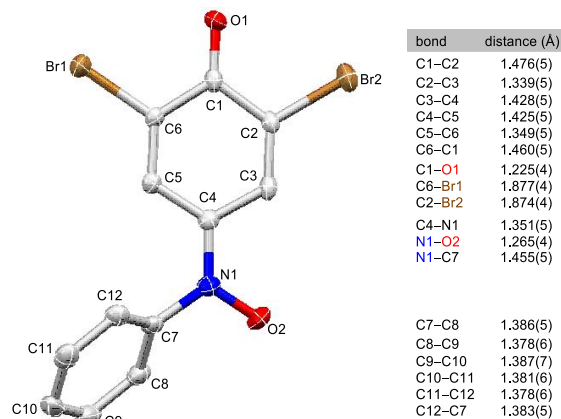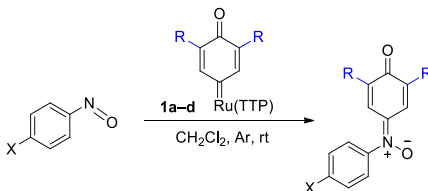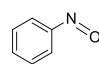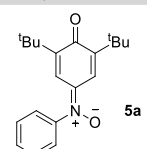

bond	distance (Å)
C1–C2	1.476(5)
C2–C3	1.339(5)
C3–C4	1.428(5)
C4–C5	1.425(5)
C5–C6	1.349(5)
C6–C1	1.460(5)
C1–O1	1.225(4)
C6–Br1	1.877(4)
C2–Br2	1.874(4)
C4–N1	1.351(5)
N1–O2	1.265(4)
N1–C7	1.455(5)
C7–C8	1.386(5)
C8–C9	1.378(6)
C9–C10	1.387(7)
C10–C11	1.381(6)
C11–C12	1.378(6)
C12–C7	1.383(5)
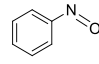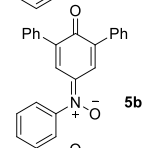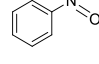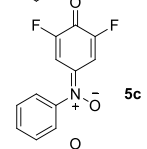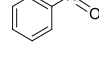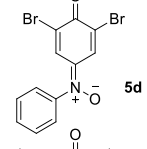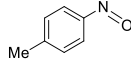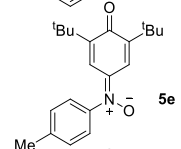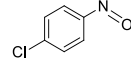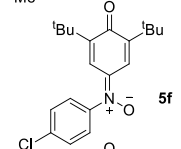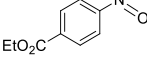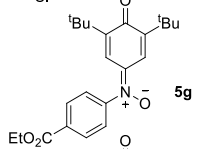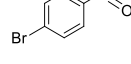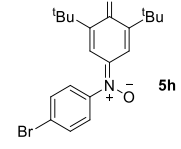
Figure 6. *ORTEP* drawing of **5d** (thermal ellipsoids at 50% probability level, hydrogen atoms not shown) and its bond distances.

We monitored the reaction between **1a** and PhNO by ^{1}H NMR spectroscopy. The time course plot showed no appreciable induction period, and the nitrone **5a** and [Ru(TTP)(PhNO)$_2$] products were cleanly formed (Figure 7). Hammett studies were then conducted for the reactions of **1a** with nitrosoarenes *p*-X-C$_6$H$_4$NO (X = Me, H, Cl, CO$_2$Et). UV-vis monitoring of the reactions between **1a** and large excess (50–200 equiv) of these nitrosoarenes gave pseudo-first-order rate constants (k_{obs}),

and the second-order rate constants (k_2) were determined by plotting k_{obs} against [ArNO] (Figure 8). By correlating the log (k_X/k_H) values with the σ_{para} values of the nitrosoarene

Table 2. Stoichiometric Reactions Between 1a–d and Nitrosoarenes

entry	nitrosoarene	product	yield (%)
1		5a	80
2		5b	87
3		5c	78
4		5d	81
5		5e	75
6		5f	88
7		5g	85
8		5h	90

Scheme 2. Stoichiometric Reaction of 3b with PhNO
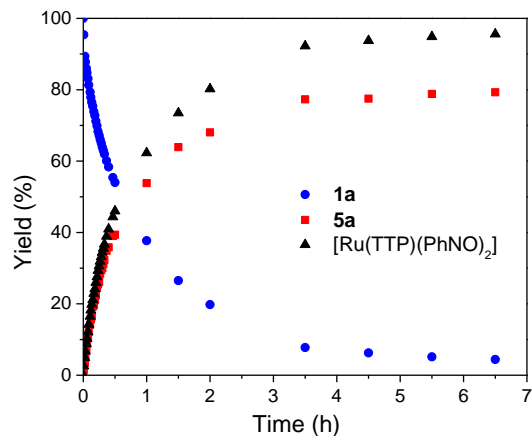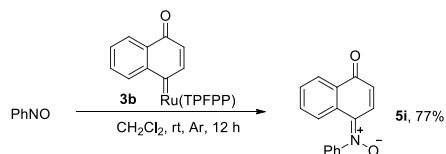
Figure 7. Time course plot of the stoichiometric reaction between **1a** and PhNO.
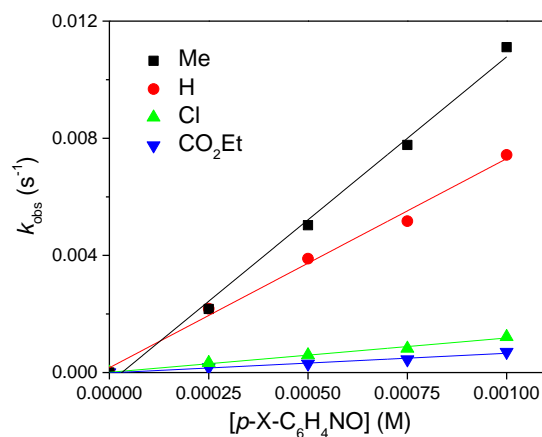
Figure 8. Plot of k_{obs} against [ArNO] for the reactions between **1a** and p-X-C_6H_4NO (X = Me, H, Cl and CO_2Et).

substituents,[30] a Hammett plot with a negative ρ value of −2.14 was obtained (Figure 9, Table S6), indicating that nitrosoarenes acted as nucleophiles in these reactions and suggesting that the coordinated QC ligand of **1a** is electrophilic.

To inspect the effect of QC substituents on the QC transfer of [Ru(Por)(QC)], we examined the kinetics of the reactions between **1a–d** and PhNO; their second-order rate constants k_2
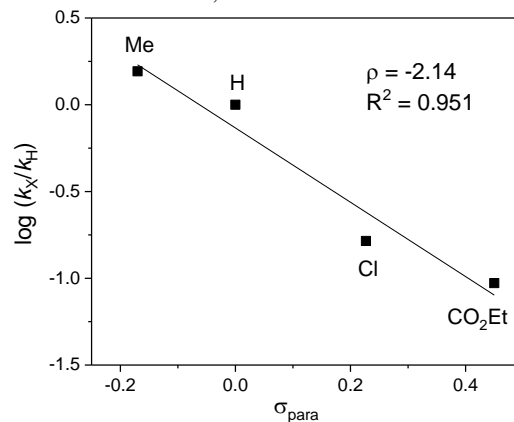
Figure 9. Hammett plot of log (k_X/k_H) against σ_{para} values of nitrosoarene substituents for the reactions between **1a** and p-X-C_6H_4NO (X = Me, H, Cl and CO_2Et).

were determined similarly from k_{obs} vs [ArNO] plots (Figure 10). The resulting log k_2 values are reasonably well correlated with the Hammett constants (σ^+_{meta}) of the substituents *meta* to the carbene carbons,[30] and a Hammett plot with, intriguingly, a negative ρ value ($\rho = -1.36$) was obtained (Figure 11, Table S7), indicating that increase of electron-withdrawing power of the substituent on the electrophilic QC lowers its reaction rate.

Figure 10. Plots of k_{obs} against [PhNO] for the reactions between **1a–d** and PhNO.

Figure 11. Hammett plot of log k_2 vs σ^+_{meta} values of QC substituents (bottom) for the reactions between **1a–d** and PhNO.

The reactivity of these Ru-QC complexes with other nucleophiles, including styrene, indole and anisole, was also tested using **1a** as example. Complex **1a** was foun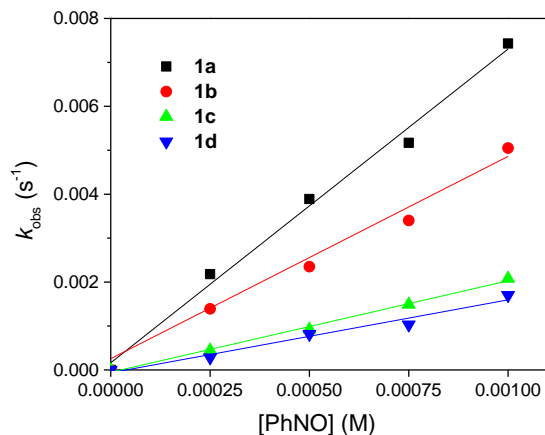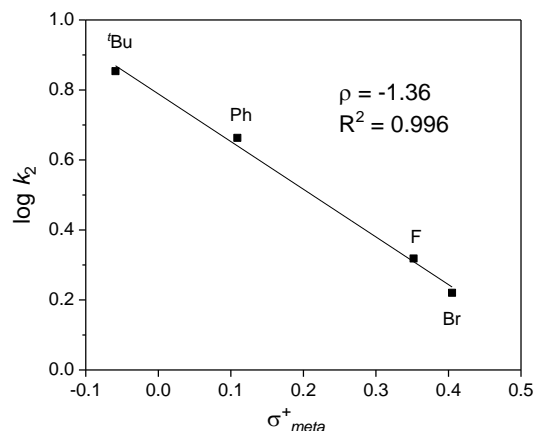d unreactive towards these nucleophiles, and no reaction occurred even at 80 °C for 24 h; addition of coordinating additives (e.g. pyridine) to the reaction mixture caused decomposition of **1a** without detectable formation of the desired QC transfer products.

Upon observation of the stoichiometric nitrone formation reactions between **1a–d** and nitrosoarenes (Table 2), and considering the formation of **1a–d** from reaction of [Ru(TTP)(CO)] with diazo quinones N_2QC^R (Scheme 1), we developed [Ru(TTP)(CO)]-catalyzed reaction of nitrosoarenes with N_2QC^R to afford nitrones (Table 3). The reaction of N_2QC^{Br} with PhNO (1.2 equiv) in the presence of [Ru(TTP)(CO)] (2 mol %) at room temperature was rather sluggish; elevation of the reaction temperature to 40 °C gave nitrone **5d** in 51% yield (Table S10). Under similar conditions

at 40 °C, a series of nitrones **5a–i** were obtained in moderate yields (30–57%) from the reactions of nitrosoarenes with diazo quinones catalyzed by [Ru(TTP)(CO)] (Table 3 and Scheme 3).

Given the above-mentioned intriguing effect of QC substituent on the rate of the stoichiometric reactions (Figure 11), we examined the corresponding QC substituent effect in the catalytic reactions. The [Ru(TTP)(CO)]-catalyzed reactions of N_2QC^R (R = ^tBu, Ph, F and Br) with PhNO were traced by ^{1}H NMR spectroscopy (time required for complete reaction: 10 h for N_2QC^{tBu}, 36 h for N_2QC^{Ph}, 52 h for N_2QC^F, 60 h for N_2QC^{Br}) and their initial rates (r_{int}) were also recorded. A good

Table 3. Reactions of Diazo Quinones N_2QC^R and Nitrosoarenes Catalyzed by [Ru(TTP)(CO)]

entry	nitrosoarene	product	yield (%)
1		**5a**	57
2		**5b**	47
3		**5c**	55
4		**5d**	51
5		**5e**	30
6		**5f**	41
7		**5g**	47
8		**5h**	45

Scheme 3. Reaction of N₂QC^Naph with PhNO Catalyzed by [Ru(TTP)(CO)]
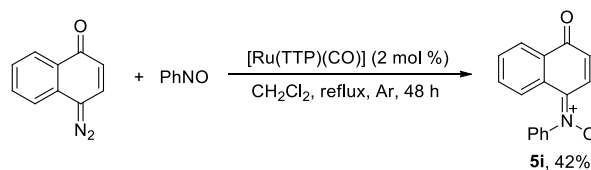
linearity was achieved when plotting the log r_{int} values (Table S8) against the Hammett constants, giving a negative ρ value of −1.66 (Figure 12) comparable to that obtained for the stoichiometric counterparts (ρ = −1.36, Figure 11).
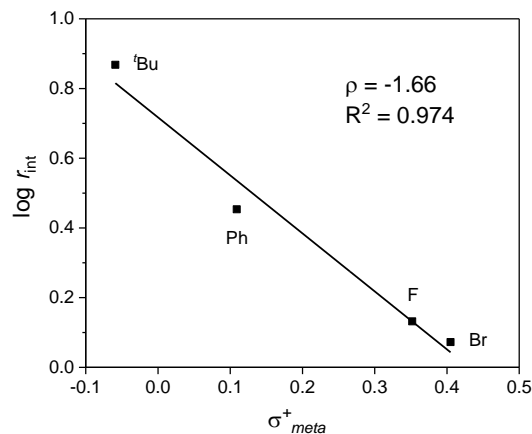
Figure 12. Hammett plot of log r_{int} vs σ^+_{meta} values of QC substituents for the [Ru(TTP)(CO)]-catalyzed reactions of N₂QC^R (R = ^tBu, Ph, F and Br) with PhNO.

(ii) HAT Reactions with C–H or X–H Substrates (X = S, N) and Catalytic Aerobic Oxidation. Metal-catalyzed carbene insertion into C–H bonds is an appealing method of C–H functionalization.[1] The reactivity of [Ru(Por)(QC^R)] towards C–H bonds was also explored. For example, treatment of [Ru(TDCPP)(QC^Br)] (**4**) with 20-fold excess of 1,4-cyclohexadiene (CHD) at room temperature for 24 h afforded benzene in 88% yield (Table 4, entry 1), apparently by oxidative C–H activation of CHD; however, no QC^Br C–H insertion product was detected. After the reaction, **4** was converted to a species formulated as [Ru^III(TDCPP)(Ar^Br)] (**6**, Ar^Br = 3,5-Br₂-4-OH-C₆H₂) based on its paramagnetic ¹H NMR spectrum (see the Supporting Information) which features the H_β signal at δ −29.64 ppm (comparable to those of [Ru^III(Por)(Ar)][31]) and resembles the spectrum of [Ru^III(TDCPP)(Ph)].[31c] Also, the ESI-MS spectrum of **6** shows a cluster peak at m/z = 1240.0 consistent with its formulation. Similarly, **1d** and **2d** could react with CHD as well, affording benzene in 87% and 83% yield, respectively.

Besides CHD, a number of other C–H substrates could also react with **4**, including a substituted CHD, two natural products γ-terpinene and terpinolene, 1,4-dihydronaphthalene, 9,10-dihydroanthracene (DHA), xanthene, 2,5-dihydrofuran, and isochroman (Table 4, entries 2–9). These reactions afforded C–H bond activated/functionalized products in moderate-to-high yields (43−83%). For treatment of **4** with relatively inert substrates such as cyclohexene and ethylbenzene, no reaction occurred even at elevated temperature (80 °C).

Table 4. Stoichiometric Reactions Between 4 and C–H or X–H Substrates[a]

entry	substrate	product[b]	yield (%)[b,c]
1	(cyclohexadiene)	(benzene)	88
2	(methylcyclohexadiene)	(toluene)	80
3	(isopropyl-methyl-cyclohexadiene)	(cymene)	71
4	(terpinolene)	(cymene)	55[d]
5	(dihydronaphthalene)	(naphthalene)	77
6	(DHA)	(anthracene)	83
7	(xanthene)	(xanthone)	75[e]
8	(dihydrofuran)	(furan)	70
9	(isochroman)	(isochromanone)	43[d,e]
10	PhSH	PhS−SPh	33
11	PhNH₂	PhN=NPh	14

[a]Reaction conditions: **4** (0.01 mmol), substrate (0.2 mmol), CH₂Cl₂ or CDCl₃ (0.5 mL), 24 h, under Ar. [b]Determined by ¹H NMR or GC. [c]Yield based on **4**. [d]Reaction time is 48 h. [e]Oxygen atom of C=O group might come from trace amount of air or moisture in the reaction system.

We then examined the reactivity of **4** towards X–H substrates PhSH and PhNH₂; the reactions afforded PhS−SPh and PhN=NPh, respectively, albeit in lower yields (Table 4, entries 10 and 11). Alcohols such as ethanol and benzyl alcohol were reported to react with ferraquinone to give aldehydes and ferrahydroquinone;[11b] in contrast, treatment of such alcohols with **4** did not result in appreciable reaction. Aprotic molecules (e.g. PhSMe) and hydride sources (e.g. Et₃SiH) were also not reactive with **4**.

Kinetic studies were performed for the reaction of **4** with DHA. Under pseudo-first-order conditions, its second-order rate constant (k_2) was determined to be 0.44 ± 0.02 M⁻¹ s⁻¹ at 298 K (Figure 13), close to that of MnO₄⁻ ion (0.48 M⁻¹ s⁻¹).[32] Changing the porphyrin ligand from TDCPP of **4** to TTP (to give **1d**) and sterically encumbered TMP (to give **2d**) slightly increased the k_2 value to 1.46 ± 0.05 and 2.21 ± 0.04 M⁻¹ s⁻¹, respectively. Eyring plot of the reaction between **4** and DHA was obtained in the temperature range of 273–313 K, and the activation parameters were determined as $\Delta H^{\ddagger}$ = 14.2 ± 0.5 kcal mol⁻¹ and $\Delta S^{\ddagger}$ = −12.3 ± 1.6 cal mol⁻¹ K⁻¹ (Figure 14). Addition of Lewis acid such as Sc(OTf)₃, FeCl₃ or proton (trifluoroacetic acid), which has been shown to improve the reactivity of metal-oxo and related species,[33] did not significantly

accelerate the HAT step (Table S11), yet FeCl$_3$ was found to facilitate the anthracene formation. However, addition of BF$_3$, a non-bulky and non-redox active Lewis acid, led to an approximately 4-fold increase of the reaction rate (Table S11). With DHA-d_4 as substrate, the k_2 value of its reaction with **4** at 298 K is 0.067 ± 0.003 M^{-1} s^{-1}, from which a KIE value of 6.6 ± 0.6 was obtained, indicating involvement of C–H bond cleavage in the rate-determining step.
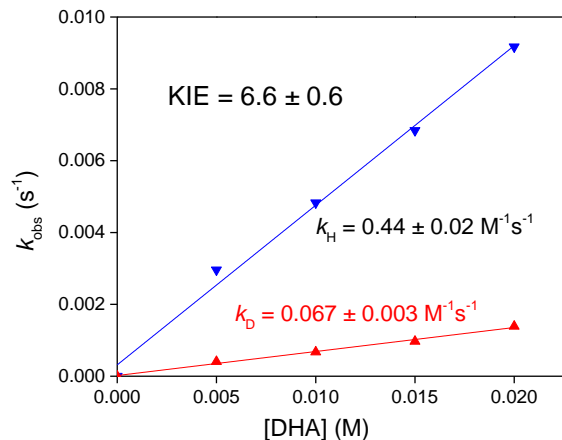

Figure 13. Plots of k_{obs} against [DHA] for the reactions of **4** with DHA and DHA-d_4 at 298 K.
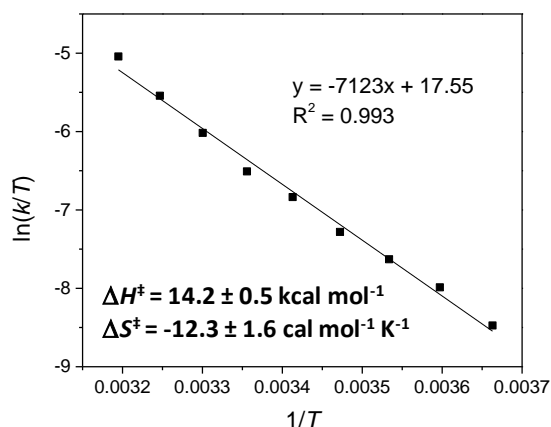

Figure 14. Eyring plot for the reaction of **4** with DHA (273–313 K).

Attempts have been made to develop a C–H activation catalysis using Ru-QC complex as catalyst. As treatment of **4** with CHD gave **6** and benzene, and **6** was found to be highly air-sensitive and could be readily converted back to **4** under aerobic conditions, the conversion of CHD to benzene could be rendered catalytic using **4** as catalyst and air as terminal oxidant. For example, treatment of CHD with catalyst **4** (0.05 mol % based on CHD) at 60 °C under aerobic conditions for 24 h gave benzene with a turnover number (TON) of 25 (Scheme 4; after the catalysis, the Ru complex(es) decomposed completely). Addition of FeCl$_3$ to the reaction mixture increased the TON to 48 (Scheme 4), but also led to a more rapid deterioration of the catalytic system (12 h).

DFT and TD-DFT Calculations. To gain further knowledge on the electronic structures of [Ru(Por)(QC)] including the influence of QC substituents, we performed

Scheme 4. Conversion of CHD to Benzene Catalyzed by 4

	additive	TON
	none	25
	FeCl$_3$ (10 mol %)	48
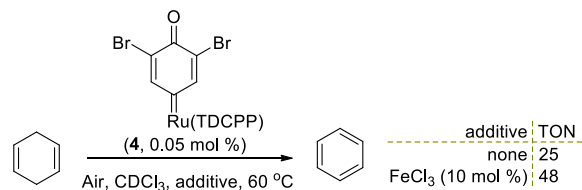
DFT/TD-DFT calculations on [Ru(TTP)(QC^R)] (R = ^{t}Bu, **1a**; Br, **1d**). The DFT-optimized structure of **1a** is consistent with its crystal structure, with the discrepancy in bond distances of the Ru-QC scaffold being ≤ 0.06 Å (Figure S13). TD-DFT calculations were conducted to simulate the UV-vis spectrum of **1a**, and the simulated spectrum compares well with the experimental one (Figure S15).

According to the MO diagram of **1a**, the bonding between Ru ion and QC ligand is rather covalent in nature, as indicated by the strong mixing in both of the corresponding π and π* orbitals (Figure 15). One of the most distinct features of QC ligand is that, it binds to the metal center through its molecular orbitals that are distributed all over the quinoid moiety, which is associated with the co-planarity of the carbonyl group with the carbene plane. This is in stark contrast to the common carbene ligands such as CPh$_2$ and C(X)CO$_2$R which mainly interact with metal centers through the p$_\pi$ atomic orbitals of the carbene carbons.[3p,q,s,v,34] The electronic transition of **1a** from Ru-carbene π (HOMO-3) to π* (LUMO) is predicted at 534 nm with moderate oscillator strength; such a transition can also be observed in the experimental UV-vis spectrum and it is mixed with the Q bands of porphyrin transitions (Figure S15). The electronic structure of **1d** is largely similar to that of **1a**, with the Ru-carbene π and π* orbitals also residing at HOMO-3 and LUMO, respectively, except that both the π and π* orbitals of **1d** are lower in energy than those of **1a** (Figure 15).
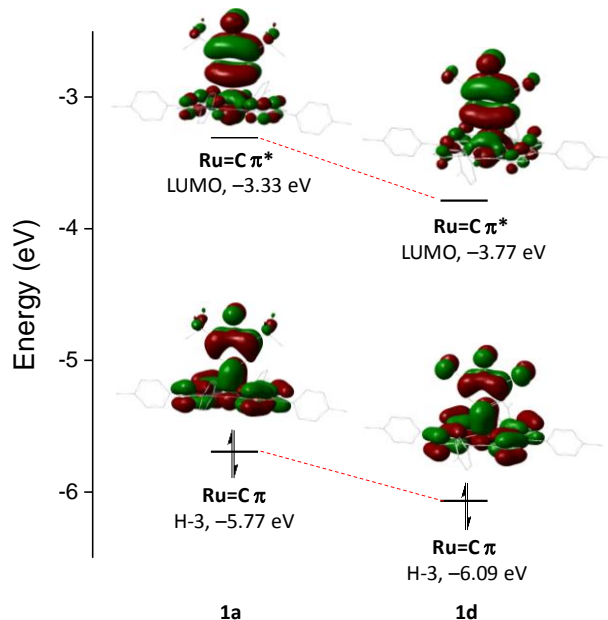

Figure 15. Comparison of calculated MO energy levels in **1a** and **1d** showing the π interactions between Ru and QC. Composition of LUMO: Ru 23%, QC^{tBu} 63%, TTP 14% for **1a**; Ru 28%, QC^{Br} 58%, TTP 14% for **1d**.

The lower energy of the π* orbital (LUMO) in **1d** than in **1a** is parallel to the experimentally measured less cathodic potential of the first reduction of **2d** than that of **2a** in the electrochemical studies (Table 1).

The mechanism of the QC transfer reaction between **1d** and PhNO was investigated by DFT calculations. As shown in the computed reaction pathway (Figure 16), PhNO prefers to directly attack the QC carbon of the five-coordinate Ru-QC complex. The reaction proceeds in a concerted manner, and the QC group becomes bent and the Ru-carbene bond starts to elongate as the nitrogen atom of PhNO approaches the carbene carbon. The transition state **TS1$_{Br}$** is predicted to be 14.2 kcal mol^{-1} higher in energy than the reactants, which is comparable to the experimental value ($\Delta G^{\ddagger}_{expt} = 17.15 \pm 0.05$ kcal mol^{-1} from $k_2 = 1.66 \pm 0.15$ M^{-1} s^{-1}). At **TS1$_{Br}$**, the Ru–C(carbene) bond is slightly lengthened to 2.02 Å (cf. 1.89 Å in **1d**), whereas the distance between carbene carbon and PhNO (1.94 Å) is much longer than the final C–N bond in **5d** (1.35 Å in both computed and crystal structures of **5d**). All these indicate a rather early transition state in this reaction. After nitrone formation, the [Ru(TTP)] moiety binds another two molecules of PhNO to afford the final [Ru(TTP)(PhNO)$_2$] product. Although axial ligand has been reported to activate metal-carbene porphyrins for carbene transfer,[4e,f] such a pathway, e.g. preformation of six-coordinate [Ru(TTP)(QC^{Br})(PhNO)] followed by attack on its carbene carbon by another PhNO molecule, is less favorable according to DFT calculations (Figure S16). The six-coordinate transition state **TS2$_{Br}$** was calculated to lie at a slightly higher energy level (15.1 kcal mol^{-1}) than **TS1$_{Br}$** (14.2 kcal mol^{-1}). In addition, the kinetic studies revealed that the rate of reaction of **1d** with PhNO is only first-order in [PhNO] (Figure 10), in disfavor of a mechanism involving participation of more than one PhNO molecules at the rate-determining step.
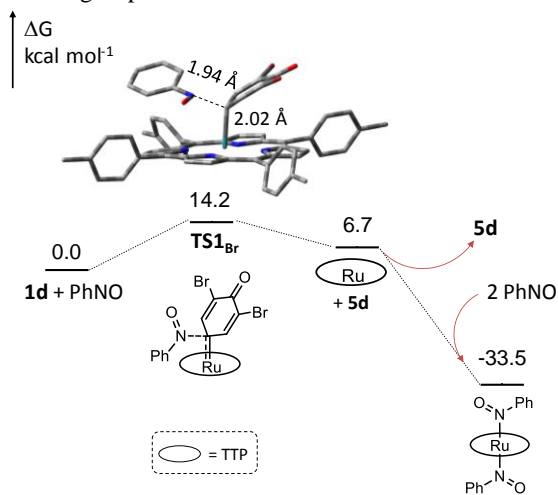

Figure 16. Computed free energy surface for the QC transfer reaction of **1d** with PhNO.

For the HAT reaction between **4** and DHA, its transition-state structure was investigated by DFT calculations (Figure 17; for other pathway, see Discussion section). The calculated barrier (17.2 kcal mol^{-1}) is in good agreement with the experimental value (17.86 ± 0.97 kcal mol^{-1} at 298 K) obtained from the Eyring plot (Figure 14). At the transition state (**TS3**),
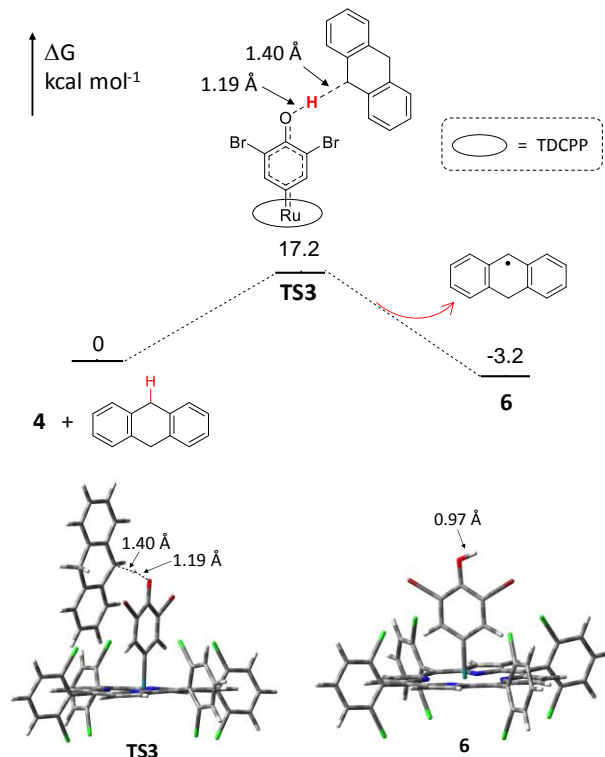
Figure 17. Computed free energy surface for the HAT reaction of **4** with DHA (above) and the DFT-optimized structures of **TS3** and **6** (bottom).

the incoming C–H bond is almost orthogonal to the QC plane, thus maximizing its overlap with the LUMO orbital of **4**. The hydrogen atom being transferred is located closer to the recipient oxygen (1.19 Å) than to the DHA molecule (1.40 Å). The O–H bond distance in **TS3** is 0.22 Å longer than that in **6**, while the reactive C–H bond in DHA is lengthened by ~0.3 Å. The product anthracene was predicted to be formed via only one transition state **TS3** without other intermediates, with the QC ligand being appreciably aromatized in **TS3** and adopting a structure approximately midway between the structures of QC and Ar ligands in **4** and **6**, respectively (Figure S18).

■ DISCUSSION

The widely proposed involvement of metal quinoid carbene (QC) intermediates in metal-catalyzed synthetically useful reactions with diazo quinones[5-9] highlights the importance of metal-QC complexes in the chemistry of QC transfer reactions. The present work, to the best of our knowledge, first demonstrates the isolation of metal-QC complexes from reactions of metal complexes with diazo quinones and the QC transfer of an isolated or directly detected metal-QC complex to organic substrates, along with structure characterization of metal-QC complexes by X-ray crystallography. Although a considerable number of isolated and/or structurally characterized metal-carbene complexes,[3,4] including those supported by porphyrin ligands,[4] can undergo carbene transfer reactions with organic substrates, their carbene ligands (such as C(Ph)CO$_2$R and CAr$_2$) are distinctly different from QCs. In the literature, examples of isolated or directly detected metal-QC complexes are extremely rare,[11] which all demonstrate a metallaquinone feature of metal-QC complexes stabilized by chelating auxilia-

ry groups on QCs with the chelating QC ligands being integrated into a quinone-like core in disfavor of QC transfer.

Remarkably, the metal-QC complexes [Ru(Por)(QC)] isolated in this work, which all feature catalytically related, monodentate QC ligands without chelating auxiliary groups, exhibit high stability yet show dual reactivity. On the basis of the experimental and DFT calculation studies performed on [Ru(Por)(QC)] in this work, the following aspects of these metal-QC complexes are discussed here.

Electronic Structures. The [Ru(Por)(QC)] complexes (**1–4**) can be described as d^6 Ru(II) species bearing neutral QC ligands, based on their NMR spectra and X-ray crystal structures and DFT calculations (see, for example, the calculated Ru d orbitals of **1a** depicted in Figure S14). Additional evidence may come from the similarity between the first oxidations of [Ru(Por)(QC)] and the well documented Ru(II)-carbonyl complexes [Ru(Por)(CO)] revealed by electrochemical and computational studies.[35] We further measured the IR spectrum of [Ru(TTP)(QC^{rBu})] (**1a**), which features an oxidation-state marker band [36] at 1010 cm^{-1} comparable to that of [Ru(TTP)(CO)] (1008 cm^{-1}), together with bands at 1653, 1593 and 1568 cm^{-1} attributable to quinoid moieties.[37]

The good stability of [Ru(Por)(QC)] in MeOH contrasts with the facile conversion of the ruthenaquinone (a Ru(0) species) to the zwitterionic Ru(II)-aryl complex in this solvent;[11a] the latter apparently originates from a 2 e$^-$ transfer from the highly reducing Ru(0) center to the chelating QC ligand. Such intramolecular Ru-to-QC electron transfer would be less favorable in the [Ru(Por)(QC)] system due to the less reducing Ru(II) center or the higher Ru(IV/II) redox potential. As to the higher stability of [Ru(TMP)(QC^R)] than that of [Ru(TTP)(QC^R)], this probably originates from the steric effect of TMP ligand, as shown by the space-filling representation of the crystal structure of **2d** (Figure S1) in which two of the *ortho*-methyl groups on the *meso*-aryl substituents are poised in front of the QC plane, thereby preventing the carbene π* orbital from being attacked by incoming molecules.

Some useful comparisons can be made between Ru-QC and Ru^{II}-NHC complexes (NHC = N-heterocyclic carbene). The isolated Ru-QC complexes, [Ru(Por)(QC)], exclusively bear mono-QC ligand, and no bis-QC complexes [Ru(Por)(QC)$_2$] were observed, unlike the isolation of bis-NHC complexes [Ru^{II}(Por)(NHC)$_2$].[38] Also, the first oxidation of [Ru(Por)(QC)] (E_{O1} = 0.28–0.54 vs Fc$^{+/0}$, Table 1) is mainly porphyrin-centered, whereas that of [Ru^{II}(Por)(NHC)$_2$] is metal-centered and with a rather low potential of $E_{1/2}$(Ru$^{III/II}$) = –0.16 vs Fc$^{+/0}$ (Por = 4-F-TPP).[38] Thus, unlike the highly electron-donating NHC ligand which tends to stabilize Ru^{III} and with relatively small trans effect, the QC ligands show large trans effect and are strong π-acceptors comparable to CO ligands. The strong π-accepting ability of the QCs could also be inferred from the observation of reductions (by cyclic voltammetry, Figure 4) ascribed to QC-centered process, which suggests low-lying carbene orbitals.

Dual Reactivity. Literature reports on dual reactivity of a metal-carbene species, such as undergoing not only carbene transfer but also other type of carbene reaction, are sparse. Examples include some traditional Fischer carbene complexes (especially Cr and W complexes) which can undergo stoichiometric transformations other than carbene transfer reaction[1g] and the metalloenolcarbenes which can be engaged in various types of cycloaddition reactions with the catalytically-active species being too unstable to be trapped or well characterized.[1p,39] For ruthenium porphyrin carbene complexes, examples that undergo stoichiometric carbene transfer reaction with organic substrates are scarce[4b,f,19] and without showing a dual carbene reactivity.

In this work, the isolated Ru(Por)(QC)] complexes display a unique substrate-dependent dual reactivity, i.e. QC transfer to nitrosoarenes and quinone-like reactivity (HAT of C−H or X−H compounds), and can be further developed into catalytic versions. Moreover, characterization of the complexes and mechanistic studies of their stoichiometric reactivities have been made possible by tuning the ligand environment. The observed reactivities of these Ru-QC complexes are probably associated with their low-lying carbene orbitals inferred from electrochemical and DFT studies. It would be of interest to build a more detailed connection between their unique reactivity pattern and their intrinsic electronic nature.

(i) QC Transfer Reactions and Effect of QC Substituents. Nitrosoarenes were found to be good substrates for the QC transfer reactions of [Ru(Por)(QC)], and the reactions led to the isolation of nitrones in up to 90% yield (Table 2). These reactions contrast with previously reported stoichiometric reactions of metal-carbene complexes (CO)$_5$M=C(OMe)Ph (M = Cr,[40b] W[40a]) with nitrosoarenes (such as PhNO) to give metathesis-like products (such as O=C(OMe)Ph and/or PhN=C(OMe)Ph),[40] rather than carbene transfer product nitrones. There is also a previous report on the stoichiometric reaction of iron-carbene complex [Cp(CO)$_2$Fe=CHAr]$^+$ (Ar = p-C$_6$H$_4$OMe) with nitrosoarenes (such as PhNO), which gave iron-nitrone complexes without resulting in the isolation of nitrones.[41]

For isolated or directly detected metal-QC complexes, the effects of QC substituents on the reactivity of their QC ligands coordinated with the same metal ion have not been reported previously. In fact, only two metal-QC complexes, a ruthenaquinone and a ferraquinone, were reported before, each bearing one chelating QC ligand.[11] In the case of free QCs, which adopt triplet ground state, introducing electron-withdrawing substituents by halogenation is reported to increases the QC's electrophilicity.[10a,42]

Considering other types of carbene ligands, the effects of carbene substituents on the reactivity of isolated metal-carbene complexes are previously focused on the reactions of M=C(X)Y (M = Cr, W; X = OR, SR, Ar; Y = Ar, OAr) complexes with nucleophiles (such as RS$^-$ and RO$^-$).[13] These reactions of electrophilic carbenes, which do not lead to carbene transfer, all feature Hammett plots with positive ρ values[13] (except for the reaction of a W=C(SR)Ar complex with HOCH$_2$CH$_2$SH[13a] described below), indicating increase of reactivity by stronger electron-withdrawing substituents and vice versa. DFT calculations on the reaction mechanism of Cr=C(X)R (X = OMe, SMe; R = Me, Ph) with nucleophile NH$_3$ also revealed a higher reaction barrier for the stronger π-donor X group.[43] In addition, previous mechanistic investigations of reactive metal-carbene complexes have been largely confined to variation of substrates and electronic/steric tuning of auxiliary ligands.[3c,j,l,m,q,u,4c,e,34f,44,45b]

With regard to carbene transfer reactions of isolated metal-carbene complexes with organic compounds, the effect of

carbene substituents on the reactivity remains rarely studied,[4e,g] despite a few reports on related systems involving in situ generated metal-carbene species in the reaction mixtures.[14,45a] For example, the reactions of $N_2C(CO_2R)C_6H_4$-*p*-R′ with alkene, Si–H or C–H substrate catalyzed by dirhodium complexes[14a,b] or [Fe(Por)Cl][14c] proceeded faster for stronger donor R′, with their Hammett plots featuring negative ρ values[14b,c] which could result from the formation of metal-carbene intermediate as the rate-determining step.[14b] Another example is the cyclopropanation of Me-OCH=CHOMe by Au(I)-carbene [IMesAu=CHC$_6$H$_4$-*p*-R]$^+$ (IMes: an NHC ligand) generated in gas phase;[45a] the reaction gave a Hammett plot with positive ρ value, which was rationalized by assuming the dissociation of the electron-rich three-membered ring as the rate-determining step.[45] Direct use of isolated metal-carbene complexes for such studies on carbene substituent effect would facilitate elucidation of their carbene transfer mechanisms.

The QC substituent effect revealed by kinetic studies on the QC transfer of [Ru(TTP)(QC^R)] (**1a−d**) with PhNO, which features a negative ρ value (Figure 11) suggestive of lower electrophilicity for stronger electron-withdrawing substituent, was quite unexpected. This reversed reactivity order, relative to that reported for free QCs[10,42] and other isolated metal-carbenes[4e,g,13] mentioned above, parallels that found in this work for the corresponding [Ru(TTP)(CO)]-catalyzed QC transfer reactions (Figure 12). Previously, the stoichiometric reaction of $(OC)_5W=C(SCH_2CH_2OH)C_6H_4$-*p*-R with $HOCH_2CH_2SH$ in $MeCN$-H_2O (1:1 v/v) was also reported to give a Hammett plot featuring a negative ρ value, which was rationalized by participation of water molecule in the transition state causing partial positive charge on the thiol S atom.[13a] In addition, there have been reports for other unusual substituent effects, such as nonlinear Hammett plots, in stoichiometric atom/group transfer reactions,[44e,46] together with reports on rare cases of inverted reactivity order in hydrogen atom abstraction by Fe^{IV}=O complexes [Fe^{IV}(O)(TMC)(X)]$^{n+}$ (TMC = tetramethylcyclam) (i.e. a higher reactivity for stronger electron-donating axial X ligand, attributed to a two-state reactivity of the Fe^{IV}=O complexes with the contribution of the more reactive state being increased by such axial ligand).[47]

To rationalize the intriguing substituent effect in the QC transfer of **1a−d** with PhNO, several factors/aspects can be considered, with steric factor being minor or ignorable in view of the large separation between the *meta*-substituents and the reaction site in the DFT-calculated transition states (see, for example, Figure 16), which is different from the cases of [Fe(Por)(CXY)] (X = H, Ph; Y = CO$_2$Et, Ph) in previously reported studies about carbene substituent effect on carbene transfer wherein a steric effect could be significant as the carbene substituents X and Y are directly bonded to the carbene carbon and thus close to the reaction site.[4e,g] Generally speaking, the electrophilicity of a coordinated carbene ligand is associated with donation from carbene to metal and insufficient π-backdonation from the metal to carbene.[48] Increasing the electron-withdrawing ability of the substituent on carbene may have several electronic effects, including: (a) lowering the electron density of free carbene, (b) reducing carbene donation to metal, (c) enhancing π-backdonation from metal to carbene, and (d) stabilizing the negative charge built up in the transition state of the attack

on carbene carbon by a nucleophile. Of these effects, (b) and (c) would reduce, whereas the others can enhance, the carbene electrophilicity/reactivity. The net effect should depend on the reaction systems including the types of metal-carbene complexes, auxiliary ligands, and the nucleophiles.

Previously reported DFT calculations on iron porphyrin complexes bearing different types of carbene ligands including CPh$_2$ and CCl$_2$ revealed that stronger electron-withdrawing carbene group causes considerably less positive charge on the carbene carbon (corresponding to markedly smaller ^{13}C NMR Fe=*C* chemical shifts), due to hindering of the carbene electron donation ability by electron-withdrawing groups.[34c] For **1a** and **1d**, which belong to the same type of carbene ligand (QC), the calculated Mulliken charges on their carbene carbons are rather similar (**1a**: −0.069; **1d**: −0.066; $\Delta q_C < 0.005$). From the ^{13}C NMR spectra of **2a–d**, their Ru=*C* chemical shifts evidently decrease with increasing electron-withdrawing ability of the QC substituent, like the cases of the iron-carbene porphyrin complexes[34c] and three-coordinate Cu=C(C{O}R)C$_6$H$_4$-*p*-R′ complexes,[3q] though different from the cases of Fe/Ru-carbene complexes [Cp(CO)(L)M=CHC$_6$H$_4$-*p*-R]$^+$ (M = Fe, Ru; L = CO, PPh$_3$).[49] This could suggests that, for [Ru(Por)(QC^R)], stronger electron-withdrawing substituent R on QC lowers the QC electrophilicity, which is likely to be associated with reduced QC-to-Ru donation and/or enhanced Ru-to-QC π-backdonation. For example, the DFT calculations suggest more pronounced Ru-to-carbene π-backdonation in **1d** than in **1a** by analyzing the component of their Ru-carbene π* orbitals (see the data in the caption of Figure 15).

We speculate that the activation barrier of the QC transfer reaction of **1a–d** with PhNO is also related to the extent of Ru-QC π-interaction and/or degree of localization of the LUMO orbital: electron-donating substituents on QC render the LUMO more localized on the carbene carbon, which can possibly facilitate its interaction with PhNO. On the other hand, in the presence of electron-withdrawing groups on QC, the Ru-QC complexes may need to undergo more reorganization processes to weaken the Ru-carbene π bond and to localize the π* orbital at the carbene carbon before the reaction can take place, thus creating a relatively higher kinetic barrier. For further comparison, besides the transition state **TS1$_{Br}$** derived from **1d** (with electron-withdrawing Br on QC), the transition state **TS1$_{tBu}$** derived from **1a** (with electron-donating ^{t}Bu on QC) was also calculated by DFT method (Figure S17). The two transition states are similar in terms of their QC structure and the chemical bonds that are breaking/forming, except that the bending angle of the quinoid plane in **TS1$_{Br}$** is ca. 10° larger than that in **TS1$_{tBu}$** (Figure 18). Possibly, as the lower-lying LUMO in **1d** results in a stronger Ru-carbene π-interaction, more bending of its QC^{Br} group is required for the partial disruption of this stronger Ru=C π bond and for the localization of LUMO to the carbene carbon; this also possibly causes a higher kinetic barrier for the reaction with **1d**. The DFT-calculated reaction barrier ($\Delta G^{\ddagger}_{calc}$) for **TS1$_{tBu}$** is 12.9 kcal mol^{-1}, which compares reasonably well with the value derived from experimentally determined k_2 value ($\Delta G^{\ddagger}_{expt}$ = 16.28 ± 0.03 kcal mol^{-1} from k_2 = 7.14 ± 0.36 M^{-1} s^{-1}); both the $\Delta G^{\ddagger}_{calc}$ and $\Delta G^{\ddagger}_{expt}$ values for **TS1$_{tBu}$**
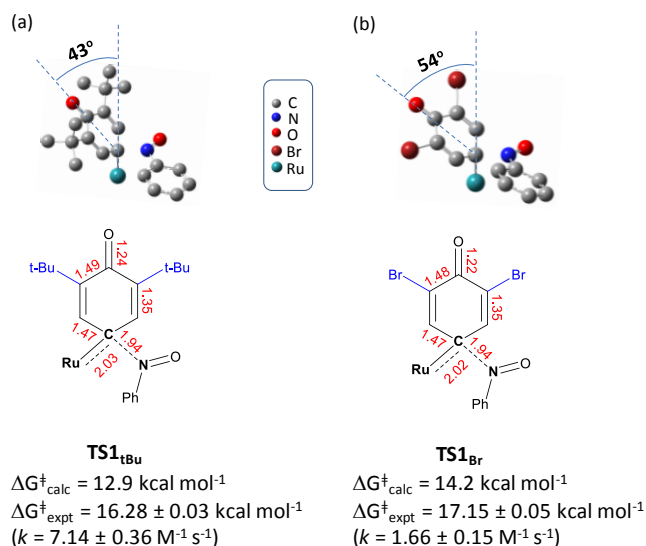
Figure 18. Comparison of DFT-calculated structures for (a) **TS1$_{tBu}$** and (b) **TS1$_{Br}$**.

are smaller than the corresponding ones for **TS1$_{Br}$** (Figure 18), consistent with the higher QC transfer reactivity observed for **1a**.

Interestingly, for the QC transfer reactions of **1a–d** with PhNO, a fair correlation can be established between the experimentally obtained carbene chemical shifts and stoichiometric/catalytic kinetics (Figure 19). This correlation links the electronic properties (characterization data) of isolated metal-QC complexes to their stoichiometric and the corresponding catalytic carbene transfer reactivities (kinetic data).
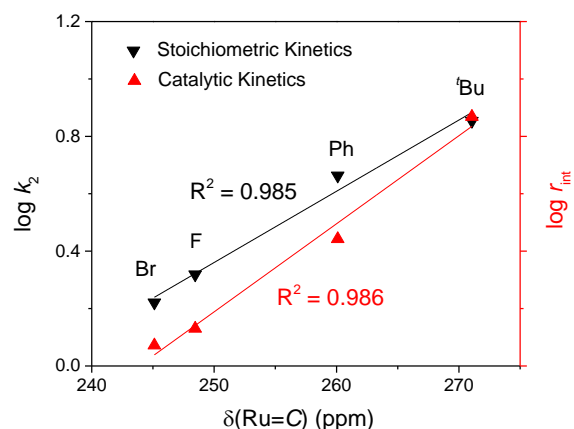

Figure 19. Correlation of kinetic data from stoichiometric and catalytic reactions with Ru=*C* ^{13}C NMR chemical shifts.

(ii) HAT Reactivity. One of the well-known reactivities of conventional metal-carbene complexes/intermediates is their carbene transfer reactions with C–H and X–H (e.g. X = N, O, S, Si) substrates, resulting in carbene insertion into these bonds.[1,2] Such carbene insertion reactions have not been observed for the [Ru(Por)(QC)] (**1–4**) complexes, despite their QC transfer reactions with nitrosoarenes. The observed interesting quinone-like HAT reactivity of these Ru-QC complexes with C–H and X–H substrates (Table 4) should stem from the unique metallaquinone[11] feature of the Ru-QC complexes. As

the QC ligands in our case are monodentate, unlike the chelating QC ligands in the previously reported metallaquinones (in which the metal-QC coordination is apparently assisted/enhanced by chelating auxiliary groups on the QC ligands),[11] the present work could demonstrate an "intrinsic" metallaquinone feature of a metal-QC complex.

Redox properties of quinone compounds have been well documented in the literature.[50] For the Ru-QC complexes, the reduction waves in their cyclic voltammograms (e.g. Figure 4) attributable to QC-based process could account for their HAT reactivity with C–H and X–H substrates. On the basis of the reaction of **4** with CHD to give **6** and benzene, together with the facile conversion of **6** to **4** by air oxidation, a mechanism was proposed for the HAT reactivity of **4**, along with resemblance of the **4**/**6** redox couple to the quinone/semiquinone couple (Scheme 5). The Ru(III)-aryl complex **6** is akin to the semiquinone (the phenoxy radical corresponds to a metalloradical in **6**), and it was possibly formed via HAT from CHD to the QC oxygen followed by an intramolecular metal-to-ligand redox-induced electron transfer (RIET), analogous to RIET processes reported for other metal complexes containing quinone-type ligands.[51] The DFT calculations on the mechanism of HAT between **4** and DHA (Figure 17), and also the large KIE value (6.6 ± 0.6) determined experimentally, are in accord with the proposed mechanism (Scheme 5). As the DFT calculations revealed the formation of **6** via a single transition state (**TS3**) without involving metal intermediate(s) (Figure 17), the HAT and RIET might happen concomitantly, which could also be suggested by the appreciably aromatized QC ligand in **TS3** (Figure S18).

Scheme 5. Proposed Mechanism for HAT Reaction of 4 with CHD and the 4/6 Redox Couple
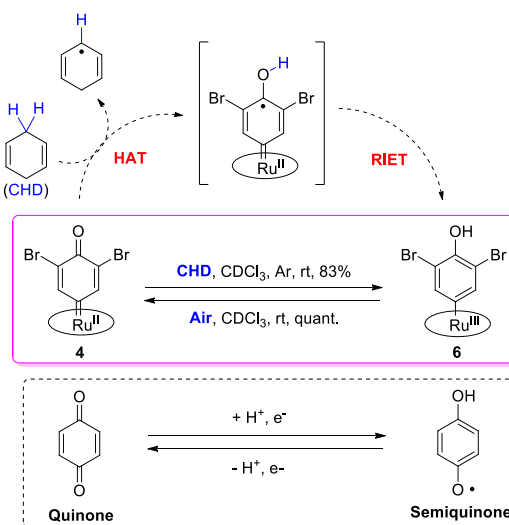
An alternative mechanistic pathway to be considered is that the carbene carbon (rather than QC oxygen) abstracts a hydrogen atom[52] from the C–H bond. For [Ru(Por)(QC)], this pathway is not favored by experimental observations, as attack on the carbene carbon would encounter much larger steric hindrance for **2d** (bearing sterically encumbered porphyrin ligand TMP) than for **1d** (bearing simple porphyrin ligand TTP), which is inconsistent with the observed higher reaction rate of DHA with **2d** than with **1d** (k_2: 2.21 ± 0.04 vs 1.46 ± 0.05 M^{-1}

s^{-1}). The higher HAT rate for **2d**, which bears a more electron-rich TMP ligand (than the TTP ligand of **1d**) and would thus be less oxidizing (see Table 1), is likely to be associated with the higher basicity of the QC group of **2d**, as HAT reactions of metal complexes depend on both of their redox potentials and the basicity of their reactive groups responsible for the HAT reactivity (for relatively low redox potentials, the basicity could play a dominant role).[53]

The reactions of **4** with C–H and X–H substrates are unlikely to proceed by a single-electron-transfer (SET) or hydride-transfer mechanism, as aprotic molecule (e.g. PhSMe) and hydride source (e.g. Et$_3$SiH) were not reactive with **4**. In addition, the finding that no QC C–H or X–H insertion products were detected in the reaction mixtures between **4** and C–H or X–H substrates demonstrates a high chemoselectivity (in terms of HAT vs carbene insertion) of these reactions.

Concerning the observed effect of Lewis acid additives such as BF$_3$ and FeCl$_3$ on the reaction of **4** with DHA and/or CHD, possible causes may be associated with the steric[33g] or redox properties of the additives, in view of the improved elementary HAT step by BF$_3$ (Table S11) and the facilitated anthracene formation (from DHA) by FeCl$_3$, but not by bulky Sc(OTf)$_3$, along with the improved product turnovers by FeCl$_3$ in the **4**-catalyzed conversion of CHD to benzene (Scheme 4). A mechanism which involves rate-limiting HAT transfer from CHD to **4** to generate a radical intermediate and reaction of the radical intermediate with air or FeCl$_3$ to give benzene (FeCl$_3$ acting as a 1 e$^-$ oxidant), could be proposed (Scheme 6; BF$_3$ was not used as an additive for the aerobic catalysis owing to its air-sensitive and non-redox active features).

Scheme 6. Proposed Mechanism for Conversion of CHD to Benzene Mediated by 4
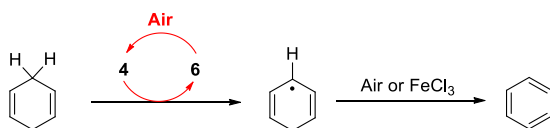
It is worth noting that the transformation of Ru-QC complex **4** to "semiquinone-like" Ru-aryl complex **6** (Scheme 5) is a net 1 e$^-$ process, unlike the 2 e$^-$-process of the ferraquinone-ferrahydroquinone couple[11b] which resembles the quinone-hydroquinone couple. Moreover, the high chemoselectivity of **4** towards HAT mechanism and much lower reactivity in other pathways differ from the oxidation reactions with quinones which have been known to proceed by various mechanisms including HAT, SET and hydride transfer.[54] In addition, the rate constant (k_2) for the DHA oxidation by **4** (0.44 ± 0.02 M^{-1} s^{-1}) is comparable to that by Ru^{VI}-oxo porphyrins [Ru^{VI}(TMP)O$_2$] (0.17 M^{-1} s^{-1}) and [Ru^{VI}(TPFPP)O$_2$] (1.74 M^{-1} s^{-1}), though smaller than that by some other Ru-oxo complexes (22–125 M^{-1} s^{-1}).[31c, 55] Different from these Ru-oxo systems which, after HAT, can undergo radical rebound to transfer the oxygen atoms to the C–H substrates,[31c,55] the QC group in **4** was transformed to an aryl ligand which is rather inert towards homolytic cleavage and radical rebound. This property of **4** renders it plausible to develop different types of metal-catalyzed C–H activation/functionalization reactions (relative to metal-oxo systems) such as the aerobic oxidation catalysis depicted in Scheme 4. Current challenges are to enhance the reactivity towards more inert C–H bonds and to improve the

stability of the catalytic system during turnover.

■ CONCLUSION

We have isolated a series of terminal monodentate quinoid carbene (QC) complexes of ruthenium, [Ru(Por)(QC)] (**1**–**4**), which were prepared using diazo quinones N$_2$QC as QC sources and exhibited dual reactivity including QC transfer with organic substrates, lending evidence for the widely proposed generation of metal-QC intermediates in various metal-catalyzed QC transfer reactions of diazo quinones. These isolated Ru-QC complexes have been characterized by spectroscopic means, electrochemical measurements, and X-ray crystal structure determinations, and span various porphyrin ligands as well as a panel of QC ligands bearing electron-withdrawing and -donating substituents, which allows fine-tuning of the energy level and reactivity of the carbene group and facilitates examination of the effect of QC substituents. DFT calculations provide useful insights into the reaction mechanisms and the electronic properties of the Ru-QC complexes, including their low-lying LUMO orbitals which are spread over the whole quinoid rings. Such a highly conjugated carbene π* orbital is crucial for their dual reactivity feature, as the incoming substrate can approach either the carbene carbon or the carbonyl oxygen, depending on the nature of the substrate.

The stoichiometric QC transfer reactions of [Ru(Por)(QC)] with nucleophilic nitrosoarenes afforded nitrone products in 75–90% yields; this reactivity, along with the preparation of [Ru(Por)(QC)] from [Ru(Por)(CO)] and diazo quinones, led to the development of a [Ru(Por)(CO)]-catalyzed nitrone formation from nitrosoarenes and diazo quinones. An inverted substituent effect on carbene reactivity, compared with that for free electrophilic QCs, was revealed by kinetic studies on the stoichiometric QC transfer reactions of complexes [Ru(TTP)(QC^R)] (**1a**–**d**; R = ^{t}Bu, Ph, F, Br) with PhNO, and also by the corresponding studies on the catalytic counterparts. The inverted substituent effect of [Ru(TTP)(QC^R)] could be rationalized by electronic factors and DFT-calculated carbene orbitals and transition state structures. A structure-reactivity relationship was established between ^{13}C NMR carbene chemical shifts and stoichiometric/catalytic kinetics.

Complexes [Ru(Por)(QC)] can also react with relatively weak C–H and X–H (X = S, N) bonds and show strong preference for a HAT mechanism. The reaction of [Ru(TDCPP)(QC^{Br})] (**4**) with the C–H bond of CHD gave a semiquinone-like Ru(III)-aryl complex [Ru^{III}(TDCPP)(Ar^{Br})] (**6**) which can be readily converted back to **4** under aerobic conditions. The **4**/**6** redox couple has been utilized to develop a catalytic aerobic oxidation of CHD to benzene, demonstrating the potential application of Ru-QC complexes in metal-catalyzed aerobic C–H activation/functionalization reactions.

Discovery of new reactivities of metal-carbene complexes and elucidation of their structure-reactivity relationship are of fundamental importance for the design of novel synthetic methodologies based on metal-carbene functionalities.[56] Despite promising synthetic utility of metal-QC complexes, there is currently rather limited knowledge of such complexes or related species in the literature.[11,57] The present work, by combining isolation, characterization and stoichiometric/catalytic reactivity study, and also DFT calculations, of the novel Ru-QC porphyrin complexes, provides useful information for the

design of related catalytic systems as well as for the future research in metal-QC chemistry.

■ ASSOCIATED CONTENT

■ AUTHOR INFORMATION

Corresponding Authors

*jshuang@hku.hk
*cmche@hku.hk
Notes
The authors declare no competing financial interest.

■ ACKNOWLEDGMENT

■ REFERENCES

(1) (a) Doyle, M. P.; Forbes, D. C. Recent advances in asymmetric catalytic metal carbene transformations. *Chem. Rev.* **1998**, *98*, 911-935. (b) Herndon, J. W. Applications of carbene complexes toward organic synthesis. *Coord. Chem. Rev.* **2000**, *206*, 237-262. (c) Lebel, H.; Marcoux, J.-F.; Molinaro, C.; Charette, A. B. Stereoselective cyclopropanation reactions. *Chem. Rev.* **2003**, *103*, 977-1050. (d) Davies, H. M. L.; Beckwith, R. E. J. Catalytic enantioselective C-H activation by means of metal-carbenoid-induced C–H insertion. *Chem. Rev.* **2003**, *103*, 2861-2903. (e) Davies, H. M. L.; Manning, J. R. Catalytic C–H functionalization by metal carbenoid and nitrenoid insertion. *Nature* **2008**, *451*, 417-424. (f) Nicolas, I.; Le Maux, P.; Simonneaux, G. Asymmetric catalytic cyclopropanation reactions in water. *Coord. Chem. Rev.* **2008**, *252*, 727-735. (g) Dötz, K. H.; Stendel, J., Jr. Fischer carbene complexes in organic synthesis: metal-assisted and metal-templated reactions. *Chem. Rev.* **2009**, *109*, 3227-3274. (h) Davies, H. M. L.; Denton, J. R. Application of donor/acceptor-carbenoids to the synthesis of natural products. *Chem. Soc. Rev.* **2009**, *38*, 3061-3071. (i) Doyle, M. P.; Duffy, R.; Ratnikov, M.; Zhou, L. Catalytic carbene insertion into C–H bonds. *Chem. Rev.* **2010**, *110*, 704-724. (j) Davies, H. M. L.; Morton, D. Guiding principles for site selective and stereoselective intermolecular C–H functionalization by donor/acceptor rhodium carbenes. *Chem. Soc. Rev.* **2011**, *40*, 1857-1869. (k) Che, C.-M.; Lo, V. K.-Y.; Zhou, C.-Y.; Huang, J.-S. Selective functionalisation of saturated C–H bonds with metalloporphyrin catalysts. *Chem. Soc. Rev.* **2011**, *40*, 1950-1975. (l) Gillingham, D.; Fei, N. Catalytic X–H insertion reactions based on carbenoids. *Chem. Soc. Rev.* **2013**, *42*, 4918-4931. (m) *Contemporary Carbene Chemistry*. Moss, R. A.; Doyle, M. P. Eds.; John Wiley & Sons: Hoboken, New Jersey, 2014. (n) Davies, H. M. L.; Alford, J. S. Reactions of metallocarbenes derived from *N*-sulfonyl-1,2,3-triazoles. *Chem. Soc. Rev.* **2014**, *43*, 5151-5162. (o) Ford, A.; Miel, H.; Ring, A.; Slattery, C. N.; Maguire, A. R.; McKervey, M. A. Modern organic synthesis with α-diazocarbonyl compounds. *Chem. Rev.* **2015**, *115*, 9981-10080. (p) Cheng, Q. Q.; Deng, Y.; Lankelma, M.; Doyle, M. P. Cycloaddition reactions of enoldiazo compounds. *Chem. Soc. Rev.* **2017**, *46*, 5425-5443. (q) Fuchibe, K.; Takayama, R.; Aono, T.; Hu, J.;

Hidano, T.; Sasagawa, H.; Fujiwara, M.; Miyazaki, S.; Nadano, R.; Ichikawa, J. Regioselective syntheses of fluorinated cyclopentanone derivatives: ring construction strategy using transition-metal-difluorocarbene complexes and free difluorocarbene. *Synthesis-Stuttgart* **2018**, *50*, 514-528. (r) Simões, M. M. Q.; Gonzaga, D. T. G.; Cardoso, M. F. C.; Forezi, L. D. S. M.; Gomes, A. T. P. C.; da Silva, F. D. C.; Ferreira, V. F.; Neves, M. G. P. M. S.; Cavaleiro, J. A. S. Carbene transfer reactions catalysed by dyes of the metalloporphyrin group. *Molecules* **2018**, *23*, 792/1-792/34. (s) Vaitla, J.; Bayer, A. Sulfoxonium ylide derived metal carbenoids in organic synthesis. *Synthesis-Stuttgart* **2019**, *51*, 612-628.

(2) (a) Vougioukalakis, G. C.; Grubbs, R. H. Ruthenium-based heterocyclic carbene-coordinated olefin metathesis catalysts. *Chem. Rev.* **2010**, *110*, 1746-1787. (b) Nolan, S. P.; Clavier, H. Chemoselective olefin metathesis transformations mediated by ruthenium complexes. *Chem. Soc. Rev.* **2010**, *39*, 3305-3316. (c) Zhu, S.-F.; Zhou, Q.-L. Iron-catalyzed transformations of diazo compounds. *Natl. Sci. Rev.* **2014**, *1*, 580-603. (d) Liu, L.; Zhang, J. Gold-catalyzed transformations of α-diazocarbonyl compounds: selectivity and diversity. *Chem. Soc. Rev.* **2016**, *45*, 506-516. (e) Xia, Y.; Qiu, D.; Wang, J. Transition-metal-catalyzed cross-couplings through carbene migratory insertion. *Chem. Rev.* **2017**, *117*, 13810-13889.

(3) For examples bearing non-porphyrin ligands, see: (a) Dötz, K. H.; Fischer, E. O. Transition metal carbene complexes. XLII. Synthesis of cyclopropane derivatives from α,β-unsaturated carboxylates with the aid of transition metal carbonyl carbene complexes. *Chem. Ber.* **1972**, *105*, 1356-1367. (b) Casey, C. P.; Burkhardt, T. J. Reactions of (diphenylcarbene)pentacarbonyltungsten(0) with alkenes. Role of metal-carbene complexes in cyclopropanation and olefin metathesis reactions. *J. Am. Chem. Soc.* **1974**, *96*, 7808-7809. (c) Casey, C. P.; Tuinstra, H. E.; Saeman, M. C. Reactions of (CO)$_5$WC(Tol)$_2$ with alkenes. A model for structural selectivity in the olefin metathesis reaction. *J. Am. Chem. Soc.* **1976**, *98*, 608-609. (d) McLain, S. J.; Wood, C. D.; Schrock, R. R. Multiple metal-carbon bonds. 6. The reaction of niobium and tantalum neopentylidene complexes with simple olefins: a route to metallocyclopentanes. *J. Am. Chem. Soc.* **1977**, *99*, 3519-3520. (e) Semmelhack, M. F.; Tamura, R. Coupling of alkenes with Fischer-type alkylidene complexes of iron. *J. Am. Chem. Soc.* **1983**, *105*, 6750-6752. (f) Doyle, M. P.; Griffin, J. H.; Bagheri, V.; Dorow, R. L. Correlations between catalytic reactions of diazo compounds and stoichiometric reactions of transition-metal carbenes with alkenes. Mechanism of the cyclopropanation reaction. *Organometallics* **1984**, *3*, 53-61. (g) Casey, C. P.; Hornung, N. L.; Kosar, W. P. Intramolecular cyclopropanation and olefin metathesis reactions of (CO)$_5$W=C(OCH$_2$CH$_2$CH=CHOCH$_3$)C$_6$H$_4$-*p*-CH$_3$. *J. Am. Chem. Soc.* **1987**, *109*, 4908-4916. (h) Wienand, A.; Reissig, H.-U. Stereospecific insertion of the carbene ligand of a Fischer carbene complex into olefinic C–H bonds. *Angew. Chem., Int. Ed.* **1990**, *29*, 1129-1131. (i) Wang, S. L. B.; Su, J.; Wulff, W. D.; Hoogsteen, K. C–H insertions in the reactions of Fischer carbene complexes with ketene acetals. *J. Am. Chem. Soc.* **1992**, *114*, 10665-10666. (j) Park, S.-B.; Sakata, N.; Nishiyama, H. Aryloxycarbonylcarbene complexes of bis(oxazolinyl)pyridineruthenium as active intermediates in asymmetric catalytic cyclopropanations. *Chem.-Eur. J.* **1996**, *2*, 303-306. (k) Gunnoe, T. B.; Surgan, M.; White, P. S.; Templeton, J. L.; Casarrubios, L. Synthesis and reactivity of tungsten(II) methylene complexes. *Organometallics* **1997**, *16*, 4865-4874. (l) Barluenga, J.; Fernández-Acebes, A.; Trabanco, A. A.; Flórez, J. Diastereoselective cyclopropanation of simple alkenes by 2-phenyl- and 2-ferrocenylalkenyl Fischer carbene complexes of chromium. *J. Am. Chem. Soc.* **1997**, *119*, 7591-7592. (m) Lee, H. M.; Bianchini, C.; Jia, G.; Barbaro, P. Styrene cyclopropanation and ethyl diazoacetate dimerization catalyzed by ruthenium complexes containing chiral tridentate phosphine ligands. *Organometallics* **1999**, *18*, 1961-1966. (n) Waterman, R.; Hillhouse, G. L. Group transfer from nickel imido, phosphinidene, and carbene complexes to ethylene with formation of aziridine, phosphirane, and cyclopropane products. *J. Am. Chem. Soc.* **2003**, *125*, 13350-13351. (o) Dai, X.; Warren, T. H. Discrete bridging

and terminal copper carbenes in copper-catalyzed cyclopropanation. *J. Am. Chem. Soc.* **2004**, *126*, 10085-10094. (p) Hofmann, P.; Shishkov, I. V.; Rominger, F. Synthesis, molecular structures, and reactivity of mono- and binuclear neutral copper(I) carbenes. *Inorg. Chem.* **2008**, *47*, 11755-11762. (q) Shishkov, I. V.; Rominger, F.; Hofmann, P. Remarkably stable copper(I) α-carbonyl carbenes: synthesis, structure, and mechanistic studies of alkene cyclopropanation reactions. *Organometallics* **2009**, *28*, 1049-1059. (r) Marquard, S. L.; Bezpalko, M. W.; Foxman, B. M.; Thomas, C. M. Stoichiometric C=O bond oxidative addition of benzophenone by a discrete radical intermediate to form a cobalt(I) carbene. *J. Am. Chem. Soc.* **2013**, *135*, 6018-6021. (s) Kornecki, K. P.; Briones, J. F.; Boyar-skikh, V.; Fullilove, F.; Autschbach, J.; Schrote, K. E.; Lancaster, K. M.; Davies, H. M. L.; Berry, J. F. Direct spectroscopic characteriza-tion of a transitory dirhodium donor-acceptor carbene complex. *Science* **2013**, *342*, 351-354. (t) Werlé, C.; Goddard, R.; Fürstner, A. The first crystal structure of a reactive dirhodium carbene complex and a versatile method for the preparation of gold carbenes by rhodium-to-gold transmetalation. *Angew. Chem., Int. Ed.* **2015**, *54*, 15452-15456. (u) Werlé, C.; Goddard, R.; Philipps, P.; Farès, C.; Fürstner, A. Struc-tures of reactive donor/acceptor and donor/donor rhodium carbenes in the solid state and their implications for catalysis. *J. Am. Chem. Soc.* **2016**, *138*, 3797-3805. (v) Bellow, J. A.; Stoian, S. A.; van Tol, J.; Ozarowski, A.; Lord, R. L.; Groysman, S. Synthesis and characteriza-tion of a stable high-valent cobalt carbene complex. *J. Am. Chem. Soc.* **2016**, *138*, 5531-5534.

(4) For examples bearing porphyrin ligands, see: (a) Smith, D. A.; Reynolds, D. N.; Woo, L. K. Cyclopropanation catalyzed by osmium porphyrin complexes. *J. Am. Chem. Soc.* **1993**, *115*, 2511-2513. (b) Galardon, E.; Le Maux, P.; Toupet, L.; Simonneaux, G. Synthesis, crystal structure, and reactivity of (5,10,15,20-tetraphenylporphyrinato)ruthenium(II) (diethoxycarbonyl)carbene methanol. *Organometallics* **1998**, *17*, 565-569. (c) Li, Y.; Huang, J.-S.; Zhou, Z.-Y.; Che, C.-M. Isolation and X-ray crystal structure of an unusual biscarbene metal complex and its reactivity toward cyclopropanation and allylic C−H insertion of unfunctionalized alkenes. *J. Am. Chem. Soc.* **2001**, *123*, 4843-4844. (d) Hamaker, C. G.; Mirafzal, G. A.; Woo, L. K. Catalytic cyclopropanation with iron(II) complexes. *Organometallics* **2001**, *20*, 5171-6176. (e) Li, Y.; Huang, J.-S.; Zhou, Z.-Y.; Che, C.-M.; You, X.-Z. Remarkably stable iron porphyrins bearing nonheteroatom-stabilized carbene or (alkoxycarbonyl)carbenes: isolation, X-ray crystal structures, and carbon atom transfer reactions with hydrocarbons *J. Am. Chem. Soc.* **2002**, *124*, 13185-13193. (f) Deng, Q.-H.; Chen, J.; Huang, J.-S.; Chui, S. S.-Y.; Zhu, N.; Li, G.-Y.; Che, C.-M. Trapping reactive metal-carbene complexes by a bis-pocket porphyrin: X-ray crystal structures of Ru=CHCO₂Et and *trans*-[Ru(CHR)(CO)] species and highly selective carbenoid transfer reactions. *Chem.-Eur. J.* **2009**, *15*, 10707-10712. (g) Wei, Y.; Tinoco, A.; Steck, V.; Fasan, R.; Zhang, Y. Cyclopropanations via heme carbenes: basic mechanism and ef-fects of carbene substituent, protein axial ligand, and porphyrin sub-stitution. *J. Am. Chem. Soc.* **2018**, *140*, 1649-1662.

(5) Dao, H. T.; Baran, P. S. Quinone diazides for olefin functionalization. *Angew. Chem., Int. Ed.* **2014**, *53*, 14382-14386.

(6) For a review, see: Othman, D. I. A.; Kitamura, M. Diazonaphthoquinones: synthesis, reactions and applications. *Heterocycles* **2016**, *92*, 1761-1783.

(7) Examples of arylation reactions: (a) Kitamura, M.; Sakata, R.; Okauchi, T. Palladium-catalyzed cross-coupling reactions of 2-diazonaphthoquinones with arylboronic acids. *Tetrahedron Lett.* **2011**, *52*, 1931-1933. (b) Baral, E. R.; Lee, Y. R.; Kim, S. H. 3-Naphthylindole construction by rhodium(II)-catalyzed regioselective direct arylation of indoles with 1-diazonaphthalen-2-(1*H*)-ones. *Adv. Synth. Catal.* **2015**, *357*, 2883-2892. (c) Kitamura, M.; Takahashi, S.; Okauchi, T. Rh-catalyzed cyclization of 3-aryloxycarbonyldiazonaphthoquinones for the synthesis of β-phenylnaphthalene lactones and formal synthesis of pradimicinone. *J. Org. Chem.* **2015**, *80*, 8406-8416. (d) Zhang, S.-S.; Jiang, C.-Y.; Wu, J.-Q.; Liu, X.-G.; Li, Q.; Huang, Z.-S.; Li, D.; Wang, H. Cp*Rh(III)

and Cp*Ir(III)-catalysed redox-neutral C–H arylation with quinone diazides: quick and facile synthesis of arylated phenols. *Chem. Commun.* **2015**, *51*, 10240-10243. (e) Das, D.; Poddar, P.; Maity, S.; Samanta, R. Rhodium(III)-catalyzed C6-selective arylation of 2-pyridones and related heterocycles using quinone diazides: syntheses of heteroarylated phenols. *J. Org. Chem.* **2017**, *82*, 3612-3621. (f) Chen, R.; Cui, S. Rh(III)-catalyzed C–H activation/cyclization of benzamides and diazonaphthalen-2(1*H*)-ones for synthesis of lactones. *Org. Lett.* **2017**, *19*, 4002-4005. (g) Liu, Z.; Wu, J.-Q.; Yang, S.-D. Ir(III)-catalyzed direct C–H functionalization of arylphosphine oxides: a strategy for MOP-type ligands synthesis. *Org. Lett.* **2017**, *19*, 5434-5437. (h) Somai Magar, K. B.; Edison, T. N. J. I.; Lee, Y. R. Regioselective construction of functionalized biarylols by Fe(OTf)₃-catalyzed direct arylation of 1-diazonaphthalen-2(1*H*)-ones and their fluorescence properties. *Eur. J. Org. Chem.* **2017**, *2017*, 7046-7054. (i) Othman, D. I. A.; Otsuka, K.; Takahashi, S.; Selim, K. B.; El-Sayed, M. A.; Tantawy, A. S.; Okauchi, T.; Kitamura, M. Total synthesis of Eleuthoside A; application of Rh-catalyzed intramolecular cyclization of diazonaphthoquinone. *Synlett* **2018**, *29*, 457-462. (j) Ghosh, B.; Biswas, A.; Chakraborty, S.; Samanta, R. Rh^III-catalyzed direct C8-arylation of quinoline *N*-oxides using diazonaphthalen-2(1*H*)-ones: a practical approach towards 8-aza BINOL. *Chem.-Asian J.* **2018**, *13*, 2388-2392. (k) Wu, K.; Cao, B.; Zhou, C.-Y.; Che, C.-M. Rh^II-catalyzed intermolecular C−H arylation of aromatics with diazo quinones. *Chem.-Eur. J.* **2018**, *24*, 4815-4819. (l) Jang, Y.-S.; Woźniak, Ł.; Pedroni, J.; Cramer, N. Access to *P*- and axially chiral biaryl phosphine oxides by enantioselective Cp^XIr^III-catalyzed C–H arylations. *Angew. Chem., Int. Ed.* **2018**, *57*, 12901-12905.

(8) Examples of alkene cyclopropanation reactions: (a) Sundberg, R. J.; Baxter, E. W.; Pitts, W. J.; Ahmed-Schofield, R.; Nishiguchi, T. Synthesis of the left-hand ring of the antitumor antibiotic CC-1065 by an intramolecular carbenoid addition route. Synthesis and reactivity of 4-diazo-4,7-dihydroindol-7-ones and related compounds. *J. Org. Chem.* **1988**, *53*, 5097-5107. (b) Sundberg, R. J.; Pitts, W. J. Synthesis of cycloprop[*c*]indol-5-ones from 4-diazo-3-[*N*-(2-propenyl)amido]cyclohexadien-1-ones. Exploration of copper(I) and copper(II) complexes as catalysts. *J. Org. Chem.* **1991**, *56*, 3048-3054. (c) Boger, D. L.; Jenkins, T. J. Synthesis, X-ray structure, and properties of fluorocyclopropane analogs of the Duocarmycins incorporating the 9,9-difluoro-1,2,9,9a-tetrahydrocyclopropa[*c*]benzo[*e*]indol-4-one (F₂CBI) alkylation subunit. *J. Am. Chem. Soc.* **1996**, *118*, 8860-8870. (d) Sawada, T.; Fuerst, D. E.; Wood, J. L. Rhodium-catalyzed synthesis of a C(3) disubstituted oxindole: an approach to diazonamide A. *Tetrahedron Lett.* **2003**, *44*, 4919-4921.

(9) Other examples: (a) Kitamura, M.; Kisanuki, M.; Sakata, R.; Okauchi, T. Pd(II)-catalyzed formal O–H insertion reactions of dia-zonaphthoquinones to acetic acid: synthesis of 1,2-naphthalenediol derivatives. *Chem. Lett.* **2011**, *40*, 1129-1131. (b) Kitamura, M.; Kis-anuki, M.; Okauchi, T. Synthesis of 1,2-naphthalenediol diacetates by rhodium(II)-catalyzed reaction of 1,2-diazonaphthoquinones with acetic anhydride. *Eur. J. Org. Chem.* **2012**, 905-907. (c) Kitamura, M.; Araki, K.; Matsuzaki, H.; Okauchi, T. Rhodium-catalyzed reaction of diazonaphthoquinones and enol ethers: synthesis of dihydronaphtho-furan derivatives and α-naphthyl esters. *Eur. J. Org. Chem.* **2013**, *2013*, 5045-5049. (d) Kitamura, M.; Kisanuki, M.; Kanemura, K.; Okauchi, T. Pd(OAc)₂-catalyzed macrocyclization of 1,2-diazonaphthoquinones with cyclic ethers. *Org. Lett.* **2014**, *16*, 1554-1557. (e) Baral, E. R.; Lee, Y. R.; Kim, S. H.; Wee, Y.-J. Rh(II)-catalyzed synthetic strategy for diverse and functionalized halonaph-thalenyl ethers and esters from diazo compounds and its application to polyaromatic compounds. *Synthesis-Stuttgart* **2016**, *48*, 579-587. (f) Kitamura, M.; Otsuka, K.; Takahashi, S.; Okauchi, T. Synthesis of 1,2-naphthalenediol derivatives by Rh-catalyzed intermolecular O–H insertion reaction of 1,2-diazonaphthoquinones with water and alco-hols. *Tetrahedron Lett.* **2017**, *58*, 3508-3511.

(10) (a) Sander, W.; Bucher, G.; Wierlacher, S. Carbenes in matri-ces - spectroscopy, structure, and reactivity. *Chem. Rev.* **1993**, *93*,

16

1583-1621. (b) Reed, D. R.; Hare, M. C.; Fattahi, A.; Chung, G.; Gordon, M. S.; Kass, S. R. α,2-, α,3-, and α,4-dehydrophenol radical anions: formation, reactivity, and energetics leading to the heats of formation of α,2-, α,3-, and α,4-oxocyclohexadienylidene. *J. Am. Chem. Soc.* **2003**, *125*, 4643-4651.

(11) (a) Ashkenazi, N.; Vigalok, A.; Parthiban, S.; Ben-David, Y.; Shimon, L. J. W.; Martin, J. M. L.; Milstein, D. Discovery of the first metallaquinone. *J. Am. Chem. Soc.* **2000**, *122*, 8797-8798. (b) Dauth, A.; Gellrich, U.; Diskin-Posner, Y.; Ben-David, Y.; Milstein, D. The ferraquinone–ferrahydroquinone couple: combining quinonic and metal-based reactivity. *J. Am. Chem. Soc.* **2017**, *139*, 2799-2807.

(12) For a review on metal complexes of carbocyclic carbenes, see: Öfele, K.; Tosh, E.; Taubmann, C.; Herrmann, W. A. Carbocyclic Carbene Metal Complexes. *Chem. Rev.* **2009**, *109*, 3408-3444.

(13) (a) Bernasconi, C. F.; Ali, M. Physical organic chemistry of transition metal carbene complexes. 17. Kinetics of the reactions of (arylthioalkoxycarbene)pentacarbonyl complexes of chromium(0) and tungsten(0) with thiolate ions in aqueous acetonitrile: pK_a values of the metal-protonated tetrahedral adducts formed between carbene complexes and thiolate ion. *J. Am. Chem. Soc.* **1999**, *121*, 11384-11394. (b) Zora, M.; Li, Y.; Herndon, J. W. Coupling of cyclobutene-diones with Fischer carbene complexes: a one-step synthesis of cy-clopentenediones and/or 5-alkylidenefuranones via net insertion of the carbene unit into a C-C bond. *Organometallics* **1999**, *18*, 4429-4436. (c) Bernasconi, C. F.; Garcia-Rio, L. Physical organic chemistry of transition metal carbene complexes. 19. Kinetics of reversible alkox-ide ion addition to substituted (methoxyphenylcar-bene)pentacarbonylchromium(0) and (methoxyphenylcar-bene)pentacarbonyltungsten(0) in methanol and aqueous acetonitrile. *J. Am. Chem. Soc.* **2000**, *122*, 3821-3829. (d) Ali, M.; Dan, A.; Ray, A.; Ghosh, K. Transition metal carbene chemistry. 4. Nucleophilic attachment of DABCO to Fischer carbene complexes in MeCN. *Inorg. Chem.* **2005**, *44*, 5866-5871. (e) Bernasconi, C. F.; Michoff, M. E. Z.; de Rossi, R. H.; Granados, A. M. Kinetics of the reactions of [*p*-nitrophenoxy(phenyl)carbene]pentacarbonylchromium(0) with ar-yloxide ions, hydroxide ion, and water in aqueous acetonitrile. Con-certed or stepwise? *J. Org. Chem.* **2007**, *72*, 1285-1293. (f) Gan-gopadhyay, S.; Mistri, T.; Dolai, M.; Alam, R.; Ali, M. Chemistry of transition metal carbene complexes: nucleophilic substitution reac-tions of cyanamide anion to Fischer carbene complexes. *Dalton Trans.* **2013**, *42*, 567-576.

(14) The addition reaction of W=C(SR)C$_6$H$_4$-*p*-R′ complexes with a thiol in aqueous solution was also reported to proceed faster for electron-donating substituent on the carbene and vice versa[13a] (see Discussion section). A few "metal catalyst + N$_2$C(CO$_2$R)C$_6$H$_4$-*p*-R′" systems (which were proposed to involve metal carbene intermediates) showing higher reactivity for the diazo compounds N$_2$C(CO$_2$R)C$_6$H$_4$-*p*-R′ bearing electron-donating R′ groups (see also Discussion section): (a) Davies, H. M. L.; Panaro, S. A. Effect of rhodium carbenoid structure on cyclopropanation chemoselectivity. *Tetrahedron* **2000**, *56*, 4871-4880. (b) Qu, Z.; Shi, W.; Wang, J. A kinetic study on the pairwise competition reaction of α-diazo esters with rhodium(II) catalysts: implication for the mechanism of Rh(II)-carbene transfer. *J. Org. Chem.* **2001**, *66*, 8139-8144. (c) Mbuvi, H. M.; Woo, L. K. Catalytic C–H insertions using iron(III) porphyrin complexes. *Organometallics* **2008**, *27*, 637-645.

(15) (a) Mansuy, D.; Lange, M.; Chottard, J. C.; Bartoli, J. F.; Chevrier, B.; Weiss, R. Dichlorocarbene complexes of iron(II)-porphyrins - crystal and molecular structure of Fe(TPP)(CCl$_2$)(H$_2$O). *Angew. Chem., Int. Ed.* **1978**, *17*, 781-782. (b) Djukic, J.-P.; Smith, D. A.; Young, V. G., Jr.; Woo, L. K. Properties and molecular structures of osmium(II) porphyrin carbene complexes: (5,10,15,20-tetra-*p*-tolylporphyrinato)osmium di-*p*-tolylmethylidene and (5,10,15,20-tetra-*p*-tolylporphyrinato)osmium (trimethylsilyl)methylidene. *Or-ganometallics* **1994**, *13*, 3020-3026. (c) Simonneaux, G.; Le Maux, P. Optically active ruthenium porphyrins: chiral recognition and asym-metric catalysis. *Coord. Chem. Rev.* **2002**, *228*, 43-60. (d) Che, C.-M.; Huang, J.-S. Ruthenium and osmium porphyrin carbene complexes: synthesis, structure, and connection to the metal-mediated cyclopropanation of alkenes. *Coord. Chem. Rev.* **2002**, *231*, 151-164. (e) Che, C.-M.; Ho, C.-M.; Huang, J.-S. Metal–carbon multiple bonded complexes: carbene, vinylidene and allenylidene complexes of ruthenium and osmium supported by macrocyclic ligands. *Coord. Chem. Rev.* **2007**, *251*, 2145-2166. (f) Zhou, C.-Y.; Huang, J.-S.; Che, C.-M. Ruthenium-porphyrin-catalyzed carbenoid transfer reactions. *Synlett* **2010**, 2681-2700. (g) Lu, H.; Zhang, X. P. Catalytic C–H functionalization by metalloporphyrins: recent developments and future directions. *Chem. Soc. Rev.* **2011**, *40*, 1899-1909. (h) Intrieri, D.; Caselli, A.; Gallo, E. Cyclopropanation reactions mediated by group 9 metal porphyrin complexes. *Eur. J. Inorg. Chem.* **2011**, *2011*, 5071-5081. (i) Thompson, S. J.; Brennan, M. R.; Lee, S. Y.; Dong, G. Synthesis and applications of rhodium porphyrin complexes. *Chem. Soc. Rev.* **2018**, *47*, 929-981.

(16) (a) Reddy, A. R.; Zhou, C.-Y.; Guo, Z.; Wei, J.; Che, C.-M. Ruthenium–porphyrin-catalyzed diastereoselective intramolecular alkyl carbene insertion into C–H bonds of alkyl diazomethanes generated in situ from *N*-tosylhydrazones. *Angew. Chem., Int. Ed.* **2014**, *53*, 14175-14180. (b) Reddy, A. R.; Hao, F.; Wu, K.; Zhou, C.-Y.; Che, C.-M. Cobalt(II) porphyrin-catalyzed intramolecular cyclopropanation of N-alkyl indoles/pyrroles with alkylcarbene: efficient synthesis of polycyclic N-heterocycles. *Angew. Chem., Int. Ed.* **2016**, *55*, 1810-1815. (c) Wang, H.; Zhou, C.-Y.; Che, C.-M. Cobalt - porphyrin-catalyzed intramolecular Buchner reaction and arene cyclopropanation of in situ generated alkyl diazomethanes. *Adv. Synth. Catal.* **2017**, *359*, 2253-2258. (d) Hao, F.; Reddy, A. R.; Zhou, C.-Y.; Che, C.-M. Cobalt(II) porphyrin catalyzed cascade reaction of pyrrolyl ketones for construction of polysubstituted pyrrolizidines and pyrrolizines. *Adv. Synth. Catal.* **2018**, *360*, 1433-1438.

(17) For a review on metal complexes with diazo compounds, see: Dartiguenave, M.; Menu, M. J.; Deydier, E.; Dartiguenave, Y.; Sie-bald, H. Crystal and molecular structures of transition metal complex-es with N- and C-bonded diazoalkane ligands. *Coord. Chem. Rev.* **1998**, *178*, 623-663.

(18) (a) Brandt, L.; Wolf, J.; Werner, H. Chloro-, methyl- und hy-drido-iridiumkomplexe mit Ph$_2$CN$_2$ und anderen diazo alkan-liganden. *J. Organomet. Chem.* **1993**, *444*, 235-244. (b) Werner, H.; Mahr, N.; Wolf, J.; Fries, A.; Laubender, M.; Bleuel, E.; Garde, R.; Lahuerta, P. Synthesis, molecular structure, and reactivity of rhodium(I) complex-es with diazoalkanes and related substrates as ligands. *Organometal-lics* **2003**, *22*, 3566-3576.

(19) Le Maux, P.; Roisnel, T.; Nicolas, I.; Simonneaux, G. Isola-tion, X-ray crystal structure, and reactivity of a new C–H carbene complex of (5,10,15,20-tetraphenylporphyrinato)ruthenium(II). *Or-ganometallics* **2008**, *27*, 3037-3042.

(20) (a) Che, C.-M.; Huang, J.-S.; Lee, F.-W.; Li, Y.; Lai, T.-S.; Kwong, H.-L.; Teng, P.-F.; Lee, W.-S.; Lo, W.-C.; Peng, S.-M.; Zhou, Z.-Y. Asymmetric inter- and intramolecular cyclopropanation of alkenes catalyzed by chiral ruthenium porphyrins. Synthesis and crystal structure of a chiral metalloporphyrin carbene complex. *J. Am. Chem. Soc.* **2001**, *123*, 4119-4129. (b) Harada, T.; Wada, S.; Yuge, H.; Miyamoto, T. K. The *trans* influence of the pyridine ligand on ruthenium(II)-porphyrin-carbene complexes. *Acta Crystallogr. Sect. C* **2003**, *59*, M37-M39. (c) Li, Y.; Huang, J.-S.; Xu, G.-B.; Zhu, N.; Zhou, Z.-Y.; Che, C.-M.; Wong, K.-Y. Spectral, structural, and electrochemical properties of ruthenium porphyrin diaryl and aryl(alkoxycarbonyl) carbene complexes: influence of carbene substituents, porphyrin substituents, and *trans*-axial ligands. *Chem.-Eur. J.* **2004**, *10*, 3486-3502. (d) Hirasawa, K.; Yuge, H.; Miyamoto, T. K. Enantiomorphs of a carbene-ruthenium(II)-porphyrin complex with four 'chiral pillars'. *Acta Crystallogr. Sect. C* **2008**, *64*, M97-M100.

(21) (a) Aleksandrov, G. G.; Struchkov, Y. T.; Kalinin, D. I.; Nei-gauz, M. G. Crystalline and molecular structure of quinone π-complexes IV. 2,6-Di-*tert*-butyl-1,4-benzoquinone. *J. Struct. Chem.* **1973**, *14*, 797-803. (b) Lü, J.-M.; Rosokha, S. V.; Neretin, I. S.; Kochi, J. K. Quinones as electron acceptors. X-ray structures, spectral (EPR, UV−vis) characteristics and electron-transfer reactivities of

their reduced anion radicals as separated vs contact ion pairs. *J. Am. Chem. Soc.* **2006**, *128*, 16708-16719.

(22) (a) Malinski, T.; Chang, D.; Bottomley, L. A.; Kadish, K. M. Substituent effects on the redox reactions of *para*-substituted tetraphenylporphyrin complexes of ruthenium(II). *Inorg. Chem.* **1982**, *21*, 4248-4253. (b) Huang, C.-Y.; Yeh, W.-L.; Cheng, S.-H. Spectral and electrochemical studies of axial ligand binding reactions of carbonyl-ruthenium(II) *meso*-tetramesitylporphyrin. *J. Electroanal. Chem.* **2005**, *577*, 179-186. (c) Berkessel, A.; Ertürk, E.; Kaiser, P.; Klein, A.; Kowalczyk, R. M.; Sarkar, B. On the redox states of ruthenium porphyrin oxidation catalysts. *Dalton Trans.* **2007**, 3427-3434.

(23) (a) Groves, J. T.; Haushalter, R. C.; Nakamura, M.; Nemo, T. E.; Evans, B. J. High-valent iron-porphyrin complexes related to peroxidase and cytochrome P-450. *J. Am. Chem. Soc.* **1981**, *103*, 2884. (b) Bell, S. R.; Groves, J. T. A highly reactive P450 model compound I. *J. Am. Chem. Soc.* **2009**, *131*, 9640.

(24) (a) Wilford, J.; Archer, M. Solvent effects on the redox potentials of benzoquinone. *J. Electroanal. Chem.* **1985**, *190*, 271-277. (b) Gupta, N.; Linschitz, H. Hydrogen-bonding and protonation effects in electrochemistry of quinones in aprotic solvents. *J. Am. Chem. Soc.* **1997**, *119*, 6384-6391. (c) Quan, M.; Sanchez, D.; Wasylkiw, M. F.; Smith, D. K. Voltammetry of quinones in unbuffered aqueous solution: reassessing the roles of proton transfer and hydrogen bonding in the aqueous electrochemistry of quinones. *J. Am. Chem. Soc.* **2007**, *129*, 12847-12856.

(25) Battioni, J.-P.; Lexa, D.; Mansuy, D.; Savéant, J.-M. Reductive electrochemistry of iron-carbene porphyrins. *J. Am. Chem. Soc.* **1983**, *105*, 207-215.

(26) (a) Reddy, A. R.; Guo, Z.; Siu, F.-M.; Lok, C.-N.; Liu, F.; Yeung, K.-C.; Zhou, C.-Y.; Che, C.-M. Diastereoselective ruthenium porphyrin-catalyzed tandem nitrone formation/1,3-dipolar cycloaddition for isoxazolidines. Synthesis, in silico docking study and in vitro biological activities. *Org. Biomol. Chem.* **2012**, *10*, 9165-9174. (b) Reddy, A. R.; Zhou, C.-Y.; Che, C.-M. Ruthenium porphyrin catalyzed three-component reaction of diazo compounds, nitrosoarenes, and alkynes: an efficient approach to multifunctionalized aziridines. *Org. Lett.* **2014**, *16*, 1048-1051. (c) Wu, K.; Zhou, C.-Y.; Che, C.-M. Perfluoroalkyl aziridines with ruthenium porphyrin carbene intermediates. *Org. Lett.* **2019**, *21*, 85-89.

(27) Nitrones are useful 1,3-dipolar reagents in organic synthesis; for reviews, see: (a) Confalone, P. N.; Huie, E. M. The [3+2] nitrone–olefin cycloaddition reaction. *Organic Reactions* **2004**, *36*, 1-173. (b) Hashimoto, T.; Maruoka, K. Recent advances of catalytic asymmetric 1,3-dipolar cycloadditions. *Chem. Rev.* **2015**, *115*, 5366-5412. (c) Murahashi, S.-I.; Imada, Y. Synthesis and transformations of nitrones for organic synthesis. *Chem. Rev.* **2019**, *119*, 4684-4716.

(28) Damavandy, J. A.; Jones, R. A. Cycloaddition reactions of quinoneimine N-oxides and of fluorenoneimine N-Oxide: exocyclic nitrones conjugated with electron-withdrawing rings. *J. Chem. Soc., Perkin Trans. 1* **1981**, 712-717.

(29) Liang, J.-L.; Huang, J.-S.; Zhou, Z.-Y.; Cheung, K.-K.; Che, C.-M. Interaction between dioxoruthenium(VI) porphyrins and hydroxylamines: coordination of *N*-substituted hydroxylamine to ruthenium and X-ray crystal structures of ruthenium complexes with a unidentate nitrosoarene ligand. *Chem.-Eur. J.* **2001**, *7*, 2306-2317.

(30) Leffler, J. E.; Grunwald, E. Rates and equilibria of organic reactions: as treated by statistical, thermodynamic and extrathermodynamic methods. Courier Corp.: Mineola, NY, USA, 2013.

(31) (a) Ke, M.; Rettig, S. J.; James, B. R.; Dolphin, D. Five-co-ordinate aryl- and alkyl-ruthenium(III) porphyrin complexes, and ruthenium–carbon bond strengths. *J. Chem. Soc., Chem. Commun.* **1987**, 1110-1112. (b) Ke, M.; Sishta, C.; James, B. R.; Dolphin, D.; Sparapany, J. W.; Ibers, J. A. Synthesis and characterization of dihalogenoruthenium(IV) and diphenylruthenium(IV), and phenylruthenium(III) tetraphenylporphyrin complexes, including the crystal structure of Ru(TPP)Br$_2$. *Inorg. Chem.* **1991**, *30*, 4766-4771. (c) Shing, K.-P.; Cao, B.; Liu, Y.; Lee, H. K.; Li, M.-D.; Phillips, D.

L.; Chang, X.-Y.; Che, C.-M. Arylruthenium(III) porphyrin-catalyzed C–H oxidation and epoxidation at room temperature and [Ru^V(Por)(O)(Ph)] intermediate by spectroscopic analysis and density functional theory calculations. *J. Am. Chem. Soc.* **2018**, *140*, 7032-7042.

(32) The rate constant of 0.48 M^{-1} s^{-1} for the reaction of DHA by MnO$_4^-$ was based on the value 0.12 M^{-1} s^{-1} (corrected per reactive hydrogen of DHA) reported in Gardner, K. A.; Kuehnert, L. L.; Mayer, J. M. Hydrogen atom abstraction by permanganate: oxidations of arylalkanes in organic solvents. *Inorg. Chem.* **1997**, *36*, 2069-2078.

(33) (a) Yiu, S.-M.; Wu, Z.-B.; Mak, C.-K.; Lau, T.-C. FeCl$_3$-activated oxidation of alkanes by [Os(N)O$_3$]$^-$. *J. Am. Chem. Soc.* **2004**, *126*, 14921-14929. (b) Yiu, S.-M.; Man, W.-L.; Lau, T.-C. Efficient catalytic oxidation of alkanes by Lewis acid/[Os^{VI}(N)Cl$_4$]$^-$ using peroxides as terminal oxidants. Evidence for a metal-based active intermediate. *J. Am. Chem. Soc.* **2008**, *130*, 10821-10827. (c) Fukuzumi, S.; Morimoto, Y.; Kotani, H.; Naumov, P.; Lee, Y.-M.; Nam, W. Crystal structure of a metal ion-bound oxoiron(IV) complex and implications for biological electron transfer. *Nat. Chem.* **2010**, *2*, 756-759. (d) Du, H.; Lo, P.-K.; Hu, Z.; Liang, H.; Lau, K.-C.; Wang, Y.-N.; Lam, W. W. Y.; Lau, T.-C. Lewis acid-activated oxidation of alcohols by permanganate. *Chem. Commun.* **2011**, *47*, 7143-7145. (e) Li, F.; Van Heuvelen, K. M.; Meier, K. K.; Münck, E.; Que, L., Jr. Sc^{3+}-triggered oxoiron(IV) formation from O$_2$ and its non-heme iron(II) precursor via a Sc^{3+}–peroxo–Fe^{3+} intermediate. *J. Am. Chem. Soc.* **2013**, *135*, 10198-10201. (f) Bang, S.; Lee, Y.-M.; Hong, S.; Cho, K.-B.; Nishida, Y.; Seo, M. S.; Sarangi, R.; Fukuzumi, S.; Nam, W. Redox-inactive metal ions modulate the reactivity and oxygen release of mononuclear non-haem iron(III)–peroxo complexes. *Nat. Chem.* **2014**, *6*, 934-940. (g) Liu, Y.; Lau, T.-C. Activation of metal oxo and nitrido complexes by Lewis acids. *J. Am. Chem. Soc.* **2019**, *141*, 3755−3766.

(34) (a) Lu, H.; Dzik, W. I.; Xu, X.; Wojtas, L.; de Bruin, B.; Zhang, X. P. Experimental evidence for cobalt(III)-carbene radicals: key intermediates in cobalt(II)-based metalloradical cyclopropanation. *J. Am. Chem. Soc.* **2011**, *133*, 8518-8521. (b) Gessner, V. H.; Meier, F.; Uhrich, D.; Kaupp, M. Synthesis and bonding in carbene complexes of an unsymmetrical dilithio methandiide: a combined experimental and theoretical study. *Chem.-Eur. J.* **2013**, *19*, 16729-16739. (c) Khade, R. L.; Fan, W.; Ling, Y.; Yang, L.; Oldfield, E.; Zhang, Y. Iron porphyrin carbenes as catalytic intermediates: structures, Mössbauer and NMR spectroscopic properties, and bonding. *Angew. Chem., Int. Ed.* **2014**, *53*, 7574-7578. (d) Sharon, D. A.; Mallick, D.; Wang, B.; Shaik, S. Computation sheds insight into iron porphyrin carbenes' electronic structure, formation, and N–H insertion reactivity. *J. Am. Chem. Soc.* **2016**, *138*, 9597-9610. (e) Yamamoto, K.; Gordon, C. P.; Liao, W.-C.; Copéret, C.; Raynaud, C.; Eisenstein, O. Orbital analysis of carbon-13 chemical shift tensors reveals patterns to distinguish fischer and schrock carbenes. *Angew. Chem., Int. Ed.* **2017**, *56*, 10127-10131. (f) Zeineddine, A.; Rekhroukh, F.; Sosa Carrizo, E. D.; Mallet-Ladeira, S.; Miqueu, K.; Amgoune, A.; Bourissou, D. Isolation of a reactive tricoordinate α-oxo gold carbene complex. *Angew. Chem., Int. Ed.* **2018**, *57*, 1306-1310.

(35) For example of computational studies on [Ru(Por)(CO)], see: Antipas, A.; Buchler, J. W.; Gouterman, M.; Smith, P. D. Porphyrins. 36. Synthesis and optical and electronic properties of some ruthenium and osmium octaethylporphyrins. *J. Am. Chem. Soc.* **1978**, *100*, 3015-3024.

(36) (a) Groves, J. T.; Ahn, K.-H. Characterization of an oxoruthenium(IV) porphyrin complex. *Inorg. Chem.* **1987**, *26*, 3831. (b) Huang, J.-S.; Che, C.-M.; Poon, C.-K. Synthesis and spectroscopy of *tert*-butylimido complexes of osmium(VI) and ruthenium(VI) porphyrins. *J. Chem. Soc., Chem. Commun.* **1992**, 161-163.

(37) Hellwig, P. Infrared spectroscopic markers of quinones in proteins from the respiratory chain. *Biochim. Biophys. Acta* **2015**, *1847*, 126-133.

(38) Chan, K.-H.; Guan, X.; Lo, V. K.-Y.; Che, C.-M. Elevated catalytic activity of ruthenium(II)-porphyrin-catalyzed carbene/nitrene transfer and insertion reactions with N-heterocyclic carbene ligands. *Angew. Chem., Int. Ed.* **2014**, *53*, 2982-2987.

(39) Xu, X.; Doyle, M. P. The [3+3]-cycloaddition alternative for heterocycle syntheses: catalytically generated metalloenolcarbenes as dipolar adducts. *Acc. Chem. Res.* **2014**, *47*, 1396-1405.

(40) (a) Pilato, R. S.; Williams, G. D.; Geoffroy, G. L.; Rheingold, A. L. Metathesis-like reactions between the carbene complex (CO)$_5$W=C(OMe)Ph and organic nitroso reagents. *Inorg. Chem.* **1988**, *27*, 3665-3668. (b) Herndon, J. W.; McMullen, L. A. Metathesis and reduction reactions of nitroso compounds with metal carbenes and metal carbonyls. *J. Organomet. Chem.* **1989**, *368*, 83-101.

(41) Peng, W.-J.; Gamble, A. S.; Templeton, J. L.; Brookhart, M. Reactions of [Cp(CO)$_2$Fe=CHAr]$^+$ (Ar = *p*-C$_6$H$_4$OMe) with O=N-AR' (Ar' = C$_6$H$_5$, *p*-C$_6$H$_4$NMe$_2$) and PhN=NPh. *Inorg. Chem.* **1990**, *29*, 463-467.

(42) (a) Sander, W.; Kötting, C.; Hübert, R. Super-electrophilic carbenes and the concept of Philicity. *J. Phys. Org. Chem.* **2000**, *13*, 561-568. (b) Sander, W.; Hübert, R.; Kraka, E.; Gräfenstein, J.; Cremer, D. 4-Oxo-2,3,5,6-tetrafluorocyclohexa-2,5-dienylidene - a highly electrophilic triplet carbene. *Chem.-Eur. J.* **2000**, *6*, 4567-4579.

(43) Andrada, D. M.; Jimenez-Halla, J. O. C.; Solà, M. Mechanism of the aminolysis of Fischer alkoxy and thiocarbene complexes: a DFT study. *J. Org. Chem.* **2010**, *75*, 5821-5836.

(44) (a) Casey, C. P.; Polichnowski, S. W.; Shusterman, A. J.; Jones, C. R. Reactions of (CO)$_5$WCHC$_6$H$_5$ with alkenes. *J. Am. Chem. Soc.* **1979**, *101*, 7282-7292. (b) Brookhart, M.; Tucker, J. R.; Husk, G. R. Synthesis, spectral characterization and alkylidene-transfer reactions of electrophilic iron carbene complexes Cp(CO)(L)Fe=CHR$^+$, L = CO, P(C$_6$H$_5$)$_3$; R = CH$_3$, CH$_2$CH$_3$, CH(CH$_3$)$_2$. *J. Am. Chem. Soc.* **1983**, *105*, 258-264. (c) Russell, S. K.; Hoyt, J. M.; Bart, S. C.; Milsmann, C.; Stieber, S. C. E.; Semproni, S. P.; DeBeer, S.; Chirik, P. J. Synthesis, electronic structure and reactivity of bis(imino)pyridine iron carbene complexes: evidence for a carbene radical. *Chem. Sci.* **2014**, *5*, 1168-1174. (d) Liu, J.; Hu, L.; Wang, L.; Chen, H.; Deng, L. An iron(II) ylide complex as a masked open-shell iron alkylidene species in its alkylidene-transfer reactions with alkenes. *J. Am. Chem. Soc.* **2017**, *139*, 3876-3888. (e) Tindall, D. J.; Werlé, C.; Goddard, R.; Philipps, P.; Farès, C.; Fürstner, A. Structure and reactivity of half-sandwich Rh(+3) and Ir(+3) carbene complexes. Catalytic metathesis of azobenzene derivatives. *J. Am. Chem. Soc.* **2018**, *140*, 1884-1893.

(45) (a) Fedorov, A.; Chen, P. Electronic effects in the reactions of olefin-coordinated gold carbene complexes. *Organometallics* **2009**, *28*, 1278-1281. (b) Fedorov, A.; Chen, P. Mechanistic insights from the gas-phase reactivity of phosphorus-ylid-supported benzylidene gold complexes. *Organometallics* **2010**, *29*, 2994-3000.

(46) (a) Ho, C.; Leung, W.-H.; Che, C.-M. Kinetics of C–H bond and alkene oxidation by *trans*-dioxoruthenium(VI) porphyrins. *J. Chem. Soc., Dalton Trans.* **1991**, 2933-2939. (b) Nelson, D. W.; Gypser, A.; Ho, P. T.; Kolb, H. C.; Kondo, T.; Kwong, H.-L.; McGrath, D. V.; Rubin, A. E.; Norrby, P.-O.; Gable, K. P.; Sharpless, K. B. Toward an understanding of the high enantioselectivity in the osmium-catalyzed asymmetric dihydroxylation. 4. Electronic effects in amine-accelerated osmylations. *J. Am. Chem. Soc.* **1997**, *119*, 1840-1858. (c) Au, S.-M.; Huang, J.-S.; Yu, W.-Y.; Fung, W.-H.; Che, C.-M. Aziridination of alkenes and amidation of alkanes by bis(tosylimido)ruthenium(VI) porphyrins. A mechanistic study. *J. Am. Chem. Soc.* **1999**, *121*, 9120-9132. (d) Hennessy, E. T.; Liu, R. Y.; Iovan, D. A.; Duncan, R. A.; Betley, T. A. Iron-mediated intermolecular N-group transfer chemistry with olefinic substrates. *Chem. Sci.* **2014**, *5*, 1526-1532.

(47) (a) Sastri, C. V.; Lee, J.; Oh, K.; Lee, Y. J.; Lee, J.; Jackson, T. A.; Ray, K.; Hirao, H.; Shin, W.; Halfen, J. A.; Kim, J.; Que, L., Jr.; Shaik, S.; Nam, W. Axial ligand tuning of a nonheme iron(IV)–oxo unit for hydrogen atom abstraction. *Proc. Natl. Acad. Sci. U. S. A.* **2007**, *104*, 19181-19186. (b) Mandal, D.; Ramanan, R.; Usharani, D.; Janardanan, D.; Wang, B.; Shaik, S. How does tunneling contribute to counterintuitive H-abstraction reactivity of nonheme Fe(IV)O oxidants with alkanes? *J. Am. Chem. Soc.* **2015**, *137*, 722-733.

(48) (a) Elschenbroich, C.; Salzer, A. *Organometallics: a concise introduction*, 2nd ed.; VCH: Weinheim, Germany, 1992. (b) Cases, M.; Frenking, G.; Duran, M.; Solà, M. Molecular structure and bond characterization of the Fischer-type chromium-carbene complexes (CO)$_5$Cr=C(X)R (X = H, OH, OCH$_3$, NH$_2$, NHCH$_3$ and R = H, CH$_3$, CH=CH$_2$, Ph, C≡CH). *Organometallics* **2002**, *21*, 4182-4191. (c) Munz, D. Pushing electrons - which carbene ligand for which application? *Organometallics* **2018**, *37*, 275-289.

(49) Brookhart, M.; Studabaker, W. B.; Humphrey, M. B.; Husk, G. R. Synthesis and spectral characterization of a series of iron and ruthenium benzylidene complexes, Cp(CO)(L)M=CH(C$_6$H$_4$R)$^+$ (M = Fe, Ru; L= CO, PPh$_3$; R = *p*-H, *p*-F, *p*-CH$_3$, *p*-OCH$_3$). Barriers to aryl rotation and benzylidene transfer reactions. *Organometallics* **1989**, *8*, 132-140.

(50) (a) Huynh, M. H. V.; Meyer, T. J. Proton-coupled electron transfer. *Chem. Rev.* **2007**, *107*, 5004-5064. (b) Warren, J. J.; Tronic, T. A.; Mayer, J. M. Thermochemistry of proton-coupled electron transfer reagents and its implications. *Chem. Rev.* **2010**, *110*, 6961-7001. (c) Son, E. J.; Kim, J. H.; Kim, K.; Park, C. B. Quinone and its derivatives for energy harvesting and storage materials. *J. Mater. Chem. A* **2016**, *4*, 11179-11202. (d) Ando, Y.; Suzuki, K. Photoredox reactions of quinones. *Chem.-Eur. J.* **2018**, *24*, 15955-15964.

(51) (a) Sofen, S. R.; Ware, D. C.; Cooper, S. R.; Raymond, K. N. Structural, electrochemical, and magnetic properties of a four-membered redox series ([Cr(L$_3$)]$^{n−}$, n = 0−3) in catechol-benzoquinone complexes of chromium. *Inorg. Chem.* **1979**, *18*, 234-239. (b) Miller, J. S.; Min, K. S. Oxidation leading to reduction: redox-induced electron transfer (RIET). *Angew. Chem., Int. Ed.* **2009**, *48*, 262-272. (c) Das, A. K.; Sarkar, B.; Fiedler, J.; Zális, S.; Hartenbach, I.; Strobel, S.; Lahiri, G. K.; Kaim, W. A five-center redox system: molecular coupling of two noninnocent imino-*o*-benzoquinonato-ruthenium functions through a π acceptor bridge. *J. Am. Chem. Soc.* **2009**, *131*, 8895-8902.

(52) Chen, K.; Zhang, S.-Q.; Brandenberg, O. F.; Hong, X.; Arnold, F. H., Alternate heme ligation steers activity and selectivity in engineered cytochrome P450-catalyzed carbene-transfer reactions. *J. Am. Chem. Soc.* **2018**, *140*, 16402-16407.

(53) (a) Bím, D.; Maldonado-Domínguez, M.; Rulíšek, L.; Srnec, M. Beyond the classical thermodynamic contributions to hydrogen atom abstraction reactivity. *Proc. Natl. Acad. Sci. U. S. A.* **2018**, *115*, E10287-E10294. (b) Goetz, M. K.; Anderson, J. S. Experimental evidence for pK_a-driven asynchronicity in C–H activation by a terminal Co(III)–oxo complex. *J. Am. Chem. Soc.* **2019**, *141*, 4051-4062.

(54) Wurche, F.; Sicking, W.; Sustmann, R.; Klärner, F.-G.; Rüchardt, C. The effect of pressure on hydrogen transfer reactions with quinones. *Chem.-Eur. J.* **2004**, *10*, 2707-2721.

(55) (a) Bryant, J. R.; Mayer, J. M. Oxidation of C−H bonds by [(bpy)$_2$(py)Ru^{IV}O]$^{2+}$ occurs by hydrogen atom abstraction. *J. Am. Chem. Soc.* **2003**, *125*, 10351-10361. (b) Che, C.-M.; Zhang, J.-L.; Zhang, R.; Huang, J.-S.; Lai, T.-S.; Tsui, W.-M.; Zhou, X.-G.; Zhou, Z.-Y.; Zhu, N.; Chang, C. K. Hydrocarbon oxidation by β-halogenated dioxoruthenium(VI) porphyrin complexes: effect of reduction potential (Ru$^{VI/V}$) and C–H bond-dissociation energy on rate constants. *Chem.-Eur. J.* **2005**, *11*, 7040-7053. (c) Wang, C.; Shalyaev, K. V.; Bonchio, M.; Carofiglio, T.; Groves, J. T. Fast catalytic hydroxylation of hydrocarbons with ruthenium porphyrins. *Inorg. Chem.* **2006**, *45*, 4769-4782. (d) Che, C.-M.; Huang, J.-S. Metalloporphyrin-based oxidation systems: from biomimetic reactions to application in organic synthesis. *Chem. Commun.* **2009**, 3996-4015.

(56) For examples, see: (a) Mindiola, D. J.; Scott, J. Carbenes and alkylidenes: spot the difference. *Nat. Chem.* **2011**, *3*, 15-17. (b) Cui, P.; Iluc, V. M. Redox-induced umpolung of transition metal carbenes. *Chem. Sci.* **2015**, *6*, 7343-7354. (c) Feichtner, K.-S.; Gessner, V. H. Cooperative bond activation reactions with carbene complexes. *Chem. Commun.* **2018**, *54*, 6540-6553. (d) LaPierre, E. A.; Piers, W. E.; Gendy, C. Redox-state dependent activation of silanes and ammonia

with reverse polarity (PC$_{carbene}$P)Ni complexes: electrophilic vs. nucleophilic carbenes. *Dalton Trans.* **2018**, *47*, 16789-16797.

(57) (a) Vigalok, A.; Milstein, D. Advances in metal chemistry of quinonoid compounds: new types of interactions between metals and aromatics. *Acc. Chem. Res.* **2001**, *34*, 798-807. (b) Albrecht, M.; Stoeckli-Evans, H. Catalytically active palladium pyridylidene complexes: pyridinium ionic liquids as N-Heterocyclic carbene precursors. *Chem. Commun.* **2005**, 4705-4707. (c) Newman, C. P.; Clarkson, G. J.; Alcock, N. W.; Rourke, J. P. Carbene or zwitterion? Competition in organoplatinum complexes. *Dalton Trans.* **2006**, 3321-3325. (d) So, S.-C.; Cheung, W.-M.; Sung, H. H.-Y.; Williams, I. D.; Leung, W.-H. 4-Hydroxyaryl complexes of group 10 metals. *J. Organomet. Chem.* **2017**, *853*, 1-4.